PNAS RESEARCH ARTICLE | NEUROSCIENCE OPEN ACCESS

V2a neurons restore diaphragm function in mice following spinal cord injury

Victoria N. Jensen[a], Emily E. Huffman[b,c], Frank L. Jalufka[d], Anna L. Pritchard[e], Sarah Baumgartner[f], Ian Walling[a,g], Holly C. Gibbs[e,h], Dylan A. McCreedy[d,e,i], Warren J. Alilain[b,c], and Steven A. Crone[f,j,k,1]

Edited by Sten Grillner, Karolinska Institutet, Stockholm, Sweden; received August 7, 2023; accepted January 15, 2024

The specific roles that different types of neurons play in recovery from injury is poorly understood. Here, we show that increasing the excitability of ipsilaterally projecting, excitatory V2a neurons using designer receptors exclusively activated by designer drugs (DREADDs) restores rhythmic bursting activity to a previously paralyzed diaphragm within hours, days, or weeks following a C2 hemisection injury. Further, decreasing the excitability of V2a neurons impairs tonic diaphragm activity after injury as well as activation of inspiratory activity by chemosensory stimulation, but does not impact breathing at rest in healthy animals. By examining the patterns of muscle activity produced by modulating the excitability of V2a neurons, we provide evidence that V2a neurons supply tonic drive to phrenic circuits rather than increase rhythmic inspiratory drive at the level of the brainstem. Our results demonstrate that the V2a class of neurons contribute to recovery of respiratory function following injury. We propose that altering V2a excitability is a potential strategy to prevent respiratory motor failure and promote recovery of breathing following spinal cord injury.

spinal cord injury | breathing | neuroplasticity | electromyography | V2a neuron

Significance

A majority of spinal cord injuries occur at the cervical level and may result in the inability to breathe without mechanical ventilation. This study shows that a genetically defined class of neuron (V2a class), that is not required for breathing in healthy rodents at rest, plays a role in recovery of breathing following injury. Increasing the excitability of V2a neurons following a C2 hemisection injury restores rhythmic inspiratory activity to the previously paralyzed hemidiaphragm. Further, silencing V2a neurons impairs activation of the paralyzed diaphragm by hypoxia/hypercapnia as well as tonic diaphragm activity observed after injury. These findings suggest that therapies to alter the excitability of V2a neurons could improve breathing following spinal cord injury.

High-level cervical spinal cord injuries disrupt connections between the brainstem respiratory centers and the respiratory motor neurons in the spinal cord and severely impair the ability to breathe. Eighty percent of deaths in patients hospitalized with cervical spinal cord injuries are due to respiratory complications, which include respiratory infections, atelectasis, and respiratory failure (1). Moreover, the number of respiratory complications contributes significantly to the length and cost of hospitalization after injury (1, 2). There are currently few treatments for respiratory dysfunction following spinal cord injury outside of mechanical ventilation and diaphragm pacing (2, 3). Neither of these strategies target the underlying deficit—the disconnect between the brainstem respiratory centers and the spinal motor neurons driving ventilation.

Plasticity within neural circuits is thought to be a major contributor to the recovery of motor function following spinal cord injury, including improvements in breathing (4–8). For example, changes in the function or connectivity of propriospinal or reticulospinal circuits are thought to contribute to improved motor function at both acute and chronic stages of injury (9–17). However, as different neurons play distinct roles in motor function (18–20) and may have distinct capacities for regeneration (21), it is important to assess which types of neurons are the strongest candidates to promote recovery of different behaviors. A recent study identified the V2a class of propriospinal neurons as a target of epidural electrical stimulation that is critical for mediating recovery of locomotor function after injury (22). Whether this class plays a role in recovery of breathing has not yet been tested.

V2a neurons are glutamatergic, ipsilaterally projecting neurons in the intermediate laminae of the spinal cord and brainstem marked by the transcription factor Chx10 (also called Vsx2) and derived from the P2 progenitor domain during development (23–26). They are distinct from the V0 class of neurons that are the core drivers of inspiration in healthy mice (27). They represent less than a third of the glutamatergic neurons in the ventral spinal cord (28). We previously showed that V2a neurons control activity of accessory respiratory muscles and enhance ventilation in healthy animals at rest (29, 30). Although V2a neuron function is not required for normal diaphragm activity in adult animals during quiet breathing (30), several studies indicate that V2a neurons may be important for recovery of diaphragm function following injury. Zholudeva *et al.* used a transsynaptic tracing technique to show that the number of V2a neurons connected to phrenic motor neurons is increased 2 wk after a C2Hx injury (31). In addition, transplanting V2a neurons along with neural progenitors improves recovery of breathing one month following a C2Hx more than transplanting neural progenitors alone (32). However, the role of endogenous V2a neurons in recovery of diaphragm function after injury has not been tested.

The C2 hemisection model (**C2Hx**) has long been used to study both functional and anatomical plasticity in respiratory circuits after injury (5, 33–38). When a hemisection is performed to lesion one half of the spinal cord at C2, the side of the diaphragm ipsilateral to the injury is paralyzed due to disrupted descending input from the brainstem pre-motor neurons to phrenic motor neurons below the injury. However, the diaphragm ipsilateral to injury can be activated within hours of

Author contributions: V.N.J., W.J.A., and S.A.C. designed research; V.N.J., E.E.H., F.L.J., A.L.P., S.B., I.W., H.C.G., and D.A.M. performed research; V.N.J., E.E.H., F.L.J., A.L.P., S.B., D.A.M., and S.A.C. analyzed data; and V.N.J., W.J.A., and S.A.C. wrote the paper.

The authors declare no competing interest.

This article is a PNAS Direct Submission.

[1]To whom correspondence may be addressed. Email: Steven.Crone@cchmc.org.

Published March 5, 2024.

injury by increasing respiratory drive. Approaches to increase respiratory drive include a phrenicotomy contralateral to the C2 hemisection (36), administration of respiratory stimulants (39), or chemosensory stimulation (40). This response, known as the "crossed phrenic phenomenon," is mediated by increased activation of spared brainstem pre-phrenic motor neurons that cross the spinal cord below the site of injury (33, 34, 41). In addition, spontaneous recovery of diaphragm function can occur weeks after injury which contributes significantly to ventilation across different levels of respiratory drive strength (42). Spontaneous recovery may be due to changes in connections between the brainstem and phrenic motor neurons, altered excitability of phrenic motor neurons, or changes in spared propriospinal circuits (4–8, 16, 17, 43, 44). Mechanical ventilation is often required in patients with cervical spinal cord injuries because spared bulbospinal pathways are insufficient to maintain adequate breathing (1, 2, 45, 46). Thus, there is a need to identify neurons or pathways that provide drive to respiratory motor neurons capable of augmenting the inspiratory drive from brainstem pre-phrenic motor neurons that are damaged by cervical injuries.

We hypothesized that V2a neurons could promote recovery of breathing at both acute and subacute (weeks later) stages following injury. To test this hypothesis, we used DREADDs (designer receptors exclusively activated by designer drugs) (47, 48) to either increase or decrease the excitability of V2a neurons acutely following a C2Hx injury to assess their role in promoting recovery of diaphragm function. Our results demonstrate that increasing V2a excitability can restore function to a paralyzed diaphragm within hours, days, or weeks after injury. We also provide evidence that V2a neurons play a role in recovery of tonic diaphragm activity following injury. Collectively, these results demonstrate that a class of ipsilaterally projecting, excitatory neurons, are capable of restoring breathing in an experimental model of respiratory plasticity. Therefore, therapies to alter the excitability or augment the function of V2a neurons may improve breathing after cervical spinal cord injury.

Results

A C2 hemisection (C2Hx) Injury Disrupts Ascending and Descending V2a Axons without Impacting V2a Neuron Survival below the Level of Injury. To assess the impact of a C2Hx injury on V2a neurons and their axons, we performed 3-dimensional lightsheet imaging of cleared brainstem-spinal cord preparations from healthy V2a-tdTomato adult mice in which V2a neurons and their processes were fluorescently labeled (Fig. 1 *A* and *B*). V2a neuron soma and axon tracts could be readily observed in lamina VII and ventral white matter of the cleared spinal cords, respectively. Using antibodies to choline acetyltransferase (ChAT) to label cholinergic neurons, we identified the phrenic motor nucleus (which contains motor neurons innervating the diaphragm) based on its location in a medial column of neurons at C4-6 in between the lateral motor column and cholinergic interneurons (near the central canal) (Fig. 1 *B* and *C*). We performed a C2Hx and imaged the spinal cord 1 d or 14 d after injury. As expected, the C2Hx disrupted V2a axons crossing the injury site (Fig. 1*C*). We manually counted axons below the injury at C5 and observed many residual tdTomato$^+$ axons after C2Hx (as shown in Fig. 1*C*) and no differences in axon numbers were detected between the contralateral and ipsilateral sides at 1 d (490.8 ± 32.3 vs. 490.2 ± 31.2) or 14 d (482.8 ± 42.3 vs. 441.4 ± 34.3) after injury. We next counted the number of V2a neuron cell bodies located at C5, well below the injury at C2. We found that there was no significant difference in the number of V2a neurons in this segment 1 or 14 d after injury compared to the uninjured cord, and no significant difference in the number of V2a neurons between the ipsilateral and contralateral side after injury (Fig. 1 *D* and *E*). Thus, despite previous studies demonstrating numerous ascending and descending V2a neuron projections between the spinal cord and brainstem (49–51), there does not appear to be a significant loss of V2a neurons or axons below the injury. Surprisingly, 3-dimensional lightsheet imaging revealed that there are rare V2a processes (axons or dendrites) that cross the midline in the cervical cord of healthy and injured mice that are not readily observed in thin tissue sections. We counted the number of V2a processes that cross the cord at C5 and found that the number of crossings does not change 1 or 14 d after C2Hx injury compared to uninjured cords (Fig. 1*F*). Thus, a C2Hx injury damages V2a axons at the site of injury but does not significantly alter the number of V2a neurons below the injury or affect the small number of V2a processes that cross the spinal cord.

The presence of V2a processes above and below the C2Hx injury (both ascending and descending) makes it challenging to assess axon tract disruption using standard imaging methods. To better assess the extent that V2a axons were disrupted by injury, we utilized fluorescence-based tractography (52) to distinguish contiguous versus disrupted V2a axons. This method uses tools developed for diffusion tractography to trace contiguous fluorescently labeled streamlines (i.e., axons or axon bundles) originating from a seed region and projecting to a target region in 3-dimensional images. Tracing streamlines originating from a seed region in C4 in the injured spinal cord shows the majority of streamlines on the ipsilateral side terminating near the C2Hx lesion, as expected, whereas the contralateral streamlines continue to ascend (Fig. 1 *G*–*I*). A small fraction of ipsilateral streamlines continued past the C2Hx injury site, suggesting some sparing of medial V2a processes/axon tracts on the injured side of the cord. To quantify sparing, we counted the number of streamlines projecting from the level of the C2Hx lesion to C4 and found a marked reduction in streamlines detected on the ipsilateral side of the spinal cord compared to the contralateral side (Fig. 1*J*). No differences were observed in the number of streamlines between the 1- and 14-d-post C2Hx groups on the ipsilateral side of the spinal cord. These results confirm that a C2Hx disrupts the majority of ascending and descending V2a axons on the side of the injury with no detectable changes in spared streamlines between 1 and 14 d after injury.

Increasing the Excitability of V2a Neurons Restores Bursting Activity to a Previously Paralyzed Diaphragm within Hours or Days Following a C2Hx Spinal Cord Injury. In order to test the impact of V2a neuron activity on diaphragm function after spinal cord injury, adult V2a-(G_q)DREADD mice (Chx10$^{Cre/+}$; ROSA$^{PNP\text{-}tTA/+}$; Tg$^{TetO\text{-}CHRM3/+}$) were generated in which the excitability of V2a neurons in the brainstem and spinal cord is increased following treatment with CNO, as previously described (29). We lesioned the left side of the spinal cord at C2 to paralyze the diaphragm ipsilateral to the injury (Fig. 2*A*). The location and completeness of each cervical lesion was assessed after the termination of the experiment by histological staining (cresyl violet) of cervical spinal cord sections (Fig. 2*B*). The extent of injury to white and gray matter is expressed as the percent of the cord that contains injured tissue in the region of maximal damage. There was no significant difference between V2a-(G_q)DREADD mice and non-DREADD-expressing controls in the amount of injured gray matter (30.3 ± 4.4% DREADD vs. 27.1 ± 4.8% non-DREADD; *t* test, $P = 0.698$) or white matter (26.3 ± 5.0% DREADD vs. 29.2 ± 4.9% non-DREADD; *t*-test, $P = 0.748$) 1 d following injury. Likewise, there was no significant difference between the extent of injury to gray matter (36.5 ± 2.0% vs. 30.3 ± 4.4%; t-test, $P = 0.863$) and white matter (29.9 ± 1.0% vs. 26.3 ± 5.0%; *t*-test, $P = 0.884$) in V2a-(Gq) DREADD mice at 4 h vs. 1 d after injury. Thus, the extent of injury was consistent between groups.

In freely breathing animals under isoflurane anesthesia, diaphragm function was assessed by surgically exposing the muscle and recording electromyography (**EMG**) from the ipsilateral and contralateral diaphragm (relative to the side of the C2Hx) 1 d following injury. The lesion was sufficient to produce complete paralysis of the diaphragm ipsilateral to the lesion during a 10-min baseline recording prior to CNO treatment (Fig. 2*C*). CNO (1.0 mg/kg*bw) was then administered to increase the excitability of V2a neurons and diaphragm EMG activity assessed for 1 h. We observed rhythmic bursting activity in the previously paralyzed ipsilateral diaphragm in 100% of animals following CNO treatment (n = 9) (Fig. 2 *C*–*E*). Diaphragm bursting continued until termination of the experiment 1 h after CNO administration. To demonstrate that the observed effects were due to activating G_q signaling in DREADD-expressing V2a neurons as opposed to off-target effects of CNO, we performed the same experiments on non-DREADD-expressing mice. The ipsilateral diaphragm remained paralyzed in 100% of non-DREADD-expressing control animals (4/4 Chx10$^{+/+}$; ROSA$^{PNP\text{-}tTA/+}$; Tg$^{TetO\text{-}CHRM3/+}$ and 3/3

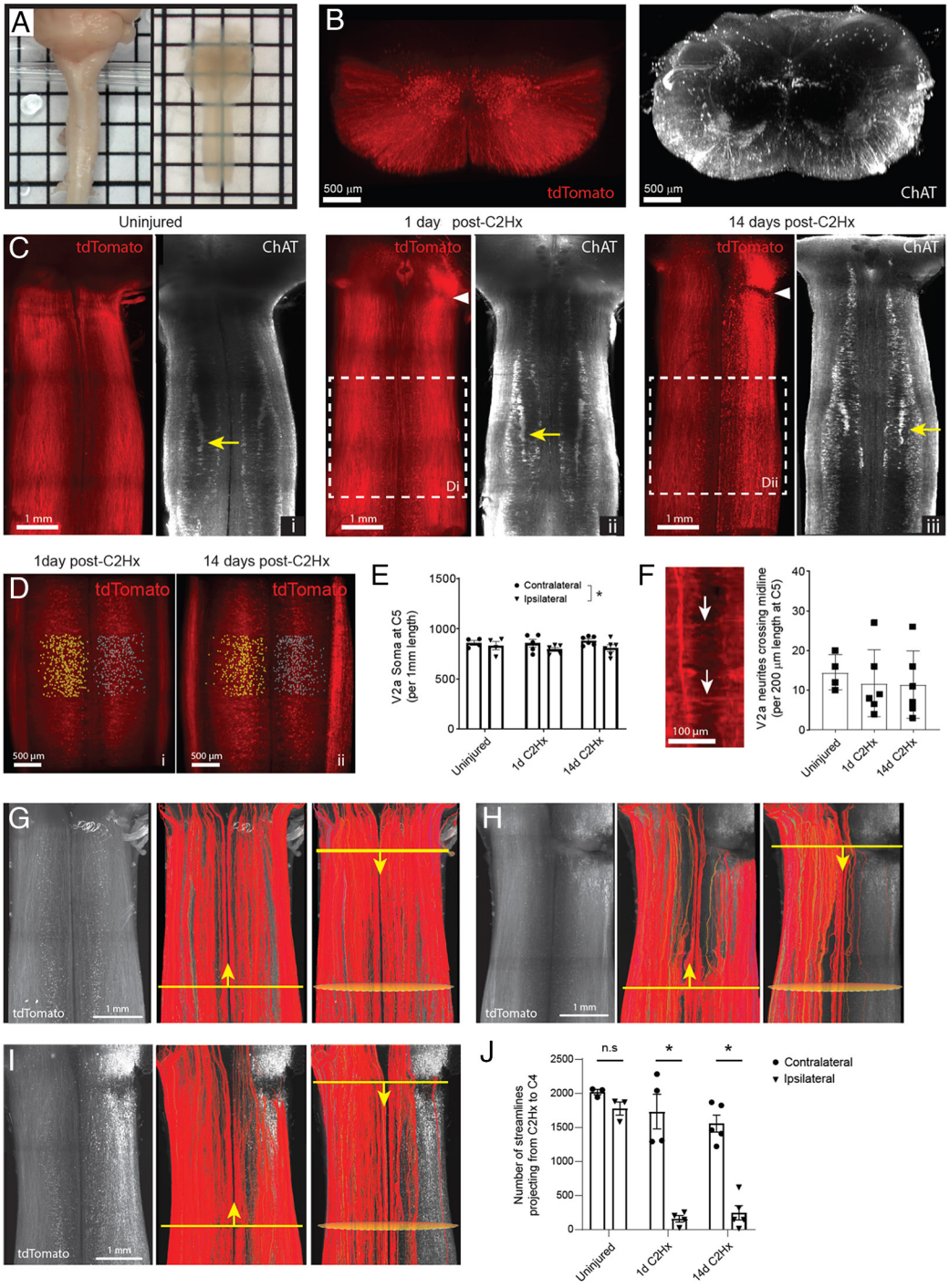

Fig. 1. Tissue clearing and 3D lightsheet imaging to assess changes in V2a neuron circuitry. (*A*) Macroscopic images of cervical spinal cords before (*Left*) and after (*Right*) tissue clearing. (*B*) 3D projection of a lightsheet image showing cross-sectional view of endogenous tdTomato fluorescence (*Left*) and ChAT immunolabeling (*Right*) in an uninjured cervical spinal cord from a V2a-tdTomato mouse. (*C*) Horizontal 3D projection of endogenous tdTomato fluorescence (*Left*) and ChAT immunolabeling (*Right*) in the uninjured cervical spinal cord (i) and at 1 d (ii) and 14 d (iii) post-C2Hx injury. The white arrowhead indicates the injury site. The yellow arrow indicates the phrenic motor pool. (*D*) V2a neuron somas counted using Imaris software on the contralateral (yellow spots) and ipsilateral (blue spots) sides of the spinal cords at C5 at 1 d (i) and 14 d (ii) post-C2Hx injury. (*E*) Total V2a neuron soma counts per 1-mm length of the spinal cord at C5. $P = 0.036$ between contralateral and ipsilateral sides across all time-points. $P > 0.19$ at each time-point. Two-way ANOVA with Sidak's multiple comparisons test. (*F*) Quantification of V2a neuron neurites crossing the midline (white arrows) per 200 µm length of the spinal cord at C5. $P = 0.81$. One-way ANOVA with Tukey's multiple comparisons test. (*G* and *H*) Fluorescence-based tractography of V2a neuron streamlines (*Left*) performed in the ascending (*Middle*) and descending (*Right*) directions in uninjured spinal cords (*G*) and at 1 d (*H*) and 14 d (*I*) post-C2Hx injury. The yellow line indicates the manually designated seed plane, and the yellow arrowhead indicates the direction of tractography. Orange ovals indicate the region of interest for quantification of streamlines. (*J*) Total number of tractography streamlines projecting from C2 to C4. $P < 0.0001$ between contralateral and ipsilateral sides at 1 d and 14 d post-C2Hx injury. Two-way ANOVA with Sidak's multiple comparisons test.

Chx10$^{Cre/+}$; ROSA$^{PNP\text{-}tTA/+}$; Tg$^{+/+}$ mice) treated with CNO (1.0 mg/kg*bw) (Fig. 2*F*). Because CNO does not differentially affect diaphragm EMG activity in Chx10$^{+/+}$; ROSA$^{PNP\text{-}tTA/+}$; Tg$^{TetO\text{-}CHRM3/+}$ and Chx10$^{Cre/+}$; ROSA$^{PNP\text{-}tTA/+}$; Tg$^{+/+}$ mice, we report the pooled data for both non-DREADD-expressing genotypes in our analyses.

We observed a decrease in frequency of inspiration over time in both DREADD-expressing and non-DREADD-expressing animals. To verify that this due to "run-down" of our anesthetized preparation as opposed to off-target effects of CNO treatment, we recorded diaphragm EMG from non-DREADD-expressing wild-type mice injected with vehicle (saline) and compared the change in frequency with that of DREADD-expressing and non-DREADD-expressing mice treated with CNO. We measured breathing frequency during a 30-s windows during the last 2 min of the baseline recording as well as 40 to 60 min after CNO or saline treatment and found a significant reduction in frequency in all groups from baseline to post-treatment in wildtype mice injected with saline (1.67 ± 0.15 Hz to 0.74 ± 0.22 Hz, n = 4, $P = 0.0007$), Non-DREADD-expressing mice treated with CNO (1.38 ± 0.53 Hz to 0.053 ± 0.33 Hz, n = 4, $P = 0.0009$), and DREADD-expressing mice treated with CNO (1.81 ± 0.45 Hz to 1.10 ± 0.28 Hz, n = 5, $P = 0.0013$), demonstrating that the decline in frequency is independent of CNO.

We next quantified the degree of recovery in V2a-(G_q)DREADD mice and controls. To control for potential differences in EMG amplitude due to variations in electrode placement in different animals (53), we normalized the EMG peak amplitude of each hemidiaphragm during the baseline (–CNO) and experimental (+CNO) periods to the EMG peak amplitude observed following maximal chemosensory stimulation, performed at the end of each recording session (Fig. 2*G*). For reference, the diaphragm EMG peak amplitude in uninjured anesthetized mice is 63% of the maximal amplitude observed during maximal chemosensory stimulation (30). As

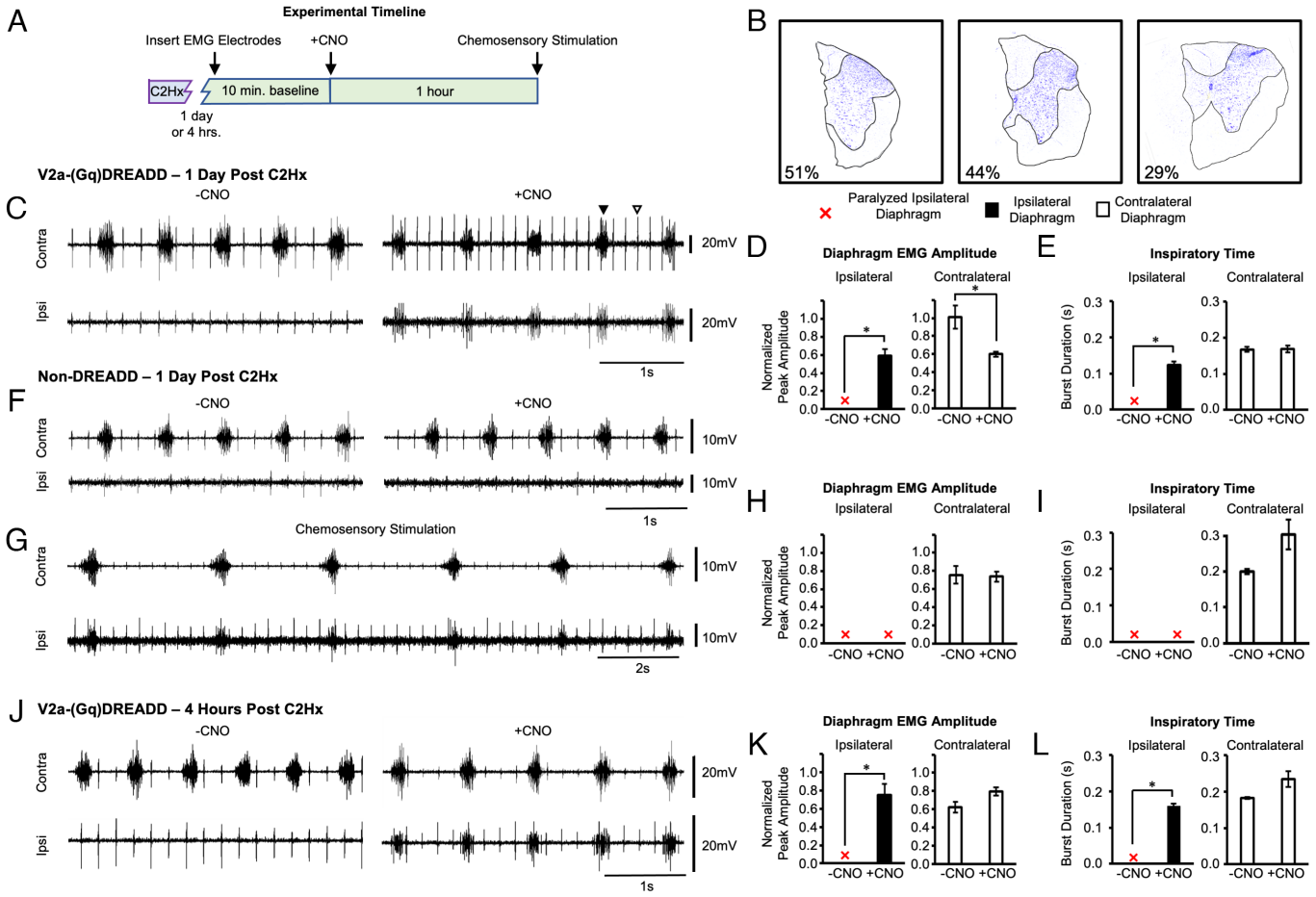

Fig. 2. Increasing the excitability of V2a neurons restores bursting activity to a previously paralyzed diaphragm within 1 d of a C2Hx injury. (*A*) Experimental timeline. V2a-(G_q)DREADD mice or non-DREADD-expressing controls received a hemisection at C2 (C2Hx). After either 4 h or 1 d, a surgical procedure was performed under anesthesia to record electromyography (EMG) from the diaphragm ipsilateral and contralateral to injury for 10 min. CNO was administered while continuously measuring diaphragm EMG for an additional hour. Chemosensory stimulation was performed to produce maximal ventilatory drive. (*B*) Representative images of C2Hx injured spinal cord sections in which neurons are stained with cresyl violet to demarcate the gray (violet, outlined) and white matter (unstained tissue, outlined). The percent of injury to the gray matter in each representative section is shown in the lower left corner. (*C*) Representative trace showing the contralateral (*Top*) and ipsilateral (*Bottom*) diaphragm before (*Left*) and after (*Right*) treatment with 1.0 mg/kg*bw CNO in a V2a-(G_q)DREADD animal 1 d post C2Hx. The diaphragm EMG peak amplitude (*D*) and inspiratory time (*E*) were measured and quantified in V2a-(G_q)DREADD mice before and after CNO treatment 1 d post C2Hx (n = 9). (*F*) Representative trace showing the contralateral (*Top*) and ipsilateral (*Bottom*) diaphragm before (*Left*) and after (*Right*) treatment with 1.0 mg/kg*bw CNO in a non-DREADD-expressing control animal. (*G*) Representative trace from a non-DREADD-expressing control animal showing that chemosensory stimulation restores bursting activity to the previously paralyzed diaphragm. The diaphragm EMG peak amplitude (*H*) and inspiratory time (*I*) were measured and quantified in all non-DREADD-expressing controls 1 d post C2Hx (n = 7). (*J*) Representative trace showing the contralateral (*Top*) and ipsilateral (*Bottom*) diaphragm before (*Left*) and after (*Right*) treatment with 1.0 mg/kg*bw CNO in a V2a-(G_q)DREADD animal 4 h after a C2Hx. The diaphragm EMG peak amplitude (*K*) and inspiratory time (*L*) were measured and quantified in V2a-(G_q)DREADD mice 4 h after a C2Hx (n = 3). White bars = contralateral diaphragm. Black bars = ipsilateral diaphragm. Red X = paralyzed ipsilateral diaphragm where no bursting activity is detected. Black arrowheads in (*C*) indicate diaphragm EMG bursts. White arrowheads in (*C*) indicate ECG activity (detected in all animals). The ipsilateral and contralateral diaphragm data were analyzed separately with a parametric paired *t*-test (*D* and *E*- contralateral, *H* and *I* and *K* and *L*) or non-parametric Wilcoxon signed-rank test (E-ipsilateral), *$P < 0.05$.

expected, all animals (DREADD expressing and non-expressing) showed rhythmic inspiratory bursting activity in the previously paralyzed diaphragm following maximal chemosensory stimulation. Note that normalization does not allow direct comparison of the ipsilateral to the contralateral diaphragm EMG peak amplitude because the EMG activity during maximal drive in the ipsilateral diaphragm is different than the contralateral diaphragm due to the injury. For this reason, we also include the raw (not normalized) EMG peak amplitude data in Table 1.

One day after a C2Hx, the diaphragm ipsilateral to injury becomes paralyzed (0% of maximal amplitude), whereas the contralateral diaphragm shows near maximal amplitude (97.5%), likely due to increased respiratory drive compensating for only one functional hemidiaphragm. CNO treatment restored activity to the ipsilateral diaphragm to 59.4% of maximal amplitude ($p<0.001$), with a corresponding decrease in contralateral diaphragm activity to 59.9% maximal amplitude (similar to pre-injury levels) ($P = 0.032$) (Fig. 2*D*). The decrease in contralateral diaphragm activity is consistent with less need for a compensatory increase in respiratory drive from the brainstem and argues against an increase in respiratory drive from the brainstem as a potential mechanism of recovery. None of the non-DREADD-expressing controls (0/7) showed recovery of diaphragm activity following CNO treatment and there was no change in the contralateral diaphragm EMG peak amplitude ($P = 0.852$) or inspiratory time ($P = 0.108$) in these animals following treatment with CNO (n = 4) (Fig. 2*H*). We found that the inspiratory time of the ipsilateral diaphragm post CNO was only 70.5% of the contralateral diaphragm post CNO (ipsi: 12.2 ± 0.7 ms vs. contra: 17.3 ± 0.7 ms, Student *t* test, $P < 0.002$), indicating that CNO treatment did not fully restore ipsilateral diaphragm activity to levels achieved in the contralateral diaphragm (Fig. 2*E*). This is consistent with observation that raw diaphragm peak EMG values of the previously paralyzed diaphragm after CNO treatment in V2a-(G_q)DREADD mice is 32% of uninjured animals (Table 1). These results show that acutely increasing the excitability of V2a neurons can restore significant function to a previously paralyzed diaphragm without increasing respiratory drive to the contralateral diaphragm.

In order to evaluate the potential of targeting V2a neurons to restore breathing shortly after a traumatic injury, we next tested whether we

Table. 1. Diaphragm EMG peak amplitude (not normalized)

Peak amplitude of rectified and integrated diaphragm EMG Average (mV) ± SEM			
V2a-(Gq)DREADD mice		−CNO	+CNO
Intact	Left	8.2 ± 1.3	8.1 ± 1.4
	Right	9.6 ± 1.2	9.1 ± 1.6
4 h Post C2Hx	Ipsi	Paralyzed	2.6 ± 0.3
	Contra	9.3 ± 0.5	12.1 ± 1.1
1 d Post C2Hx	Ipsi	Paralyzed	2.5 ± 0.8
	Contra	16.4 ± 2.0	10.1 ± 1.3
2 wk Post C2Hx - Non-recovered	Ipsi	Paralyzed	2.2 ± 0.2
	Contra	11.6 ± 2.4	11.0 ± 1.7
2 wk Post C2Hx - Recovered	Ipsi	3.1 ± 0.3	3.3 ± 0.2
	Contra	17.0 ± 0.1	16.2 ± 0.1
Non-DREADD mice		−CNO	+CNO
1 d Post C2Hx	Ipsi	Paralyzed	Paralyzed
	Contra	11.0 ± 2.3	10.2 ± 2.1
2 wk Post C2Hx - Non-recovered	Ipsi	Paralyzed	Paralyzed
	Contra	9.1 ± 0.8	9.0 ± 0.8
2 wk Post C2Hx - Recovered	Ipsi	1.9 ± 0.3	2.2 ± 0.3
	Contra	11.7 ± 0.4	9.9 ± 0.3
V2a-(Gi)DREADD mice- Chemosensory Stimulation		−CNO	+CNO
2 wk Post C2Hx - Non-Recovered	Ipsi	8.4 ± 1.3	3.3 ± 0.4
	Contra	20.1 ± 4.0	18.7 ± 4.9
V2a-(Gi)DREADD mice- Eupnea		−CNO	+CNO
2 wk Post	Ipsi	6.9 ± 1.6	5.9 ± 1.1
C2Hx- Recovered- Rhythmic	Contra	15.3 ± 1.8	17.3 ± 3.0

could achieve recovery within hours of a C2Hx. The same experimental paradigm described above was used to measure diaphragm EMG and increase the excitability of V2a neurons 4 h after injury. All of the animals (3/3) showed strong recovery of ipsilateral hemidiaphragm bursting activity following CNO treatment with an average normalized peak amplitude of 73 ± 14% maximal activity (Fig. 2*J*). Unlike animals tested 1 d following injury, the contralateral diaphragm EMG peak amplitude did not decrease as the ipsilateral diaphragm recovered function (P = 0.281) (Fig. 2*K*). Similar to the results seen in V2a-(G_q)DREADD mice tested 1 d following injury, the inspiratory time of the ipsilateral diaphragm was lower than the inspiratory time of the contralateral diaphragm (ipsi: 15.9 ± 0.8 ms vs. contra: 23.4 ± 2.0 ms, P = 0.0565) (Fig. 2*L*), suggesting that recovery is not to pre-injury levels (see also Table 1). Nevertheless, these data demonstrate that increasing the excitability of V2a neurons can restore rhythmic bursting activity to a previously paralyzed diaphragm as soon as 4 h following a C2Hx spinal cord injury.

Increasing the Excitability of V2a Neurons Restores Diaphragm Function 2 wk Following a C2Hx. Spontaneous recovery of ipsilateral diaphragm function can occur in some animals within weeks of a C2Hx injury (43, 54–57), likely due to plasticity within respiratory circuits [which may include changes in the connectivity between V2a and phrenic motor neurons (31)]. We assessed the impact of altering V2a neuron function during this subacute phase. We recorded diaphragm EMG, as described previously, 2 wk after a C2Hx injury and classified the animals into groups: "animals with recovery" (i.e., rhythmic inspiratory bursting activity is observed in ipsilateral diaphragm, 5/12 V2a-(G_q)DREADD mice) or "animals without recovery" (i.e., no inspiratory activity, 7/12 V2a-(G_q)DREADD mice). The recovery group may include animals that underwent spontaneous recovery as well as those with incomplete lesions. Note, however, that recovered animals comprised just 15% of animals 1 d after injury (presumably due to incomplete lesions). All animals showed lack of chest movement ipsilateral to injury immediately following the C2Hx, demonstrating significant impairment of respiratory function on that side at the time of injury. We found no significant difference in the anatomical extent of injury between V2a-(G_q)DREADD animals that did not show recovery versus animals that showed recovery prior to CNO treatment (Gray matter: 24.1 ± 5.6% no recovery vs. 26.1 ± 3.1% recovery, P = 0.458; White matter: 22.6 ± 5.8% no recovery vs. 26.6 ± 3.6% recovery, P = 0.337). Thus, the 2-wk time point after a C2Hx injury provides an opportunity to assess the impact of altering V2a neuron excitability on animals with different levels of functional deficits during the subacute period.

We first measured the effects of increasing the excitability of V2a neurons in the group of 7 V2a-(G_q)DREADD mice without recovery (prior to CNO treatment). CNO restored inspiratory bursting activity to the previously paralyzed ipsilateral diaphragm in all seven animals (Fig. 3 *A*–*C*). The contralateral diaphragm EMG peak amplitude was not significantly changed after CNO treatment (P = 0.895), indicating that V2a neurons are not increasing respiratory drive. In non-DREADD-expressing controls (without recovery group), CNO did not restore activity to the ipsilateral diaphragm or alter contralateral diaphragm EMG peak amplitude (n = 4, paired t-test, P = 0.895) or inspiratory time (paired t-test, P = 0.181) (Fig. 3 *D*-and *E*). Thus, increasing the excitability of V2a neurons can improve diaphragm function at subacute stages as well as acutely after injury.

We next examined the effects of increasing the excitability of V2a neurons in the group of 5 V2a-(G_q)DREADD mice that showed rhythmic inspiratory activity in the ipsilateral diaphragm prior to CNO treatment (Fig. 3*F*). Increasing the excitability of V2a neurons with CNO in these animals had no effect on the ipsilateral diaphragm EMG peak amplitude (ipsi: P = 0.229; contra: P = 0.182) or inspiratory time (ipsi: P = 0.725; contra: P = 0.520) (Fig. 3 *G* and *H*). However, we did observe an increase in tonic muscle activity in the ipsilateral diaphragm during the expiratory period in V2a-(G_q)DREADD animals treated with CNO (Fig. 3*F*), which has also been observed in uninjured V2a-(G_q)DREADD animals treated with CNO (30). Additionally, no effects of CNO on diaphragm EMG peak amplitude were observed in 5/5 non-DREADD-expressing controls that showed recovery prior to CNO treatment (Fig. 3 *I* and *J*). Thus, increasing the excitability of V2a neurons has a minimal impact on peak diaphragm activity in mice that have already recovered rhythmic inspiratory diaphragm function.

Cycle Triggered Averaging Reveals that the Predominant Pattern of Diaphragm Activity after Activating V2a Neurons Is Rhythmic Inspiratory Bursting. We observed differences in the pattern of diaphragm activity throughout the post-CNO recording period, even within individual animals. For example, tonic activity would appear and disappear over time in animals that showed tonic activity (Fig. 4*A*). In order to better characterize and quantify the different patterns of diaphragm activity observed following CNO treatment, we performed cycle triggered averaging (CTA) to correlate ipsilateral diaphragm activity with the rhythmic inspiratory burst activity observed in the contralateral diaphragm (Fig. 4). Five different CTA patterns were observed in the ipsilateral diaphragm using this analysis: 1) paralysis- characterized by a complete lack of EMG activity 2) rhythmic bursting- characterized by ipsilateral diaphragm activity only during inspiration and synchronous with contralateral diaphragm bursting activity 3) rhythmic bursting combined with tonic activity during expiration 4) tonic activity only during expiration and no activity during inspiration and 5) tonic activity during both the expiratory and inspiratory phases of respiration.

We measured the average amount of time each V2a-(G_q)DREADD mouse spent in each CTA pattern after CNO administration 4 h, 1 d, and 2 wk following the C2Hx spinal cord injury. Only V2a-(G_q)DREADD mice without recovery (prior to CNO) were included in this analysis. CTA pattern frequency analysis was initiated as soon as the first non-paralyzed CTA pattern emerged following CNO administration and the percentage of time spent in each CTA pattern was calculated. There was no difference among groups (4 h, 1 d, or 2 wk) in the amount of time it took for the first non-paralyzed CTA pattern to emerge (4 h group: 14.2 ± 5.4 min vs. 1-d group: 18.7 ± 4.5 min vs. 2-week group: 8.7 ± 2.0 min, one-way ANOVA, P = 0.266). Most of the time was spent in the rhythmic-only bursting pattern for all three time points after injury (Fig. 4*G*). However, the fraction of time spent in the rhythmic-only bursting pattern was significantly greater in the 2 wk and 1 d post injury group compared to the 4 h post injury group (two-way ANOVA, Bonferroni post-hoc test, P < 0.05 in both comparisons). These data demonstrate that rhythmic

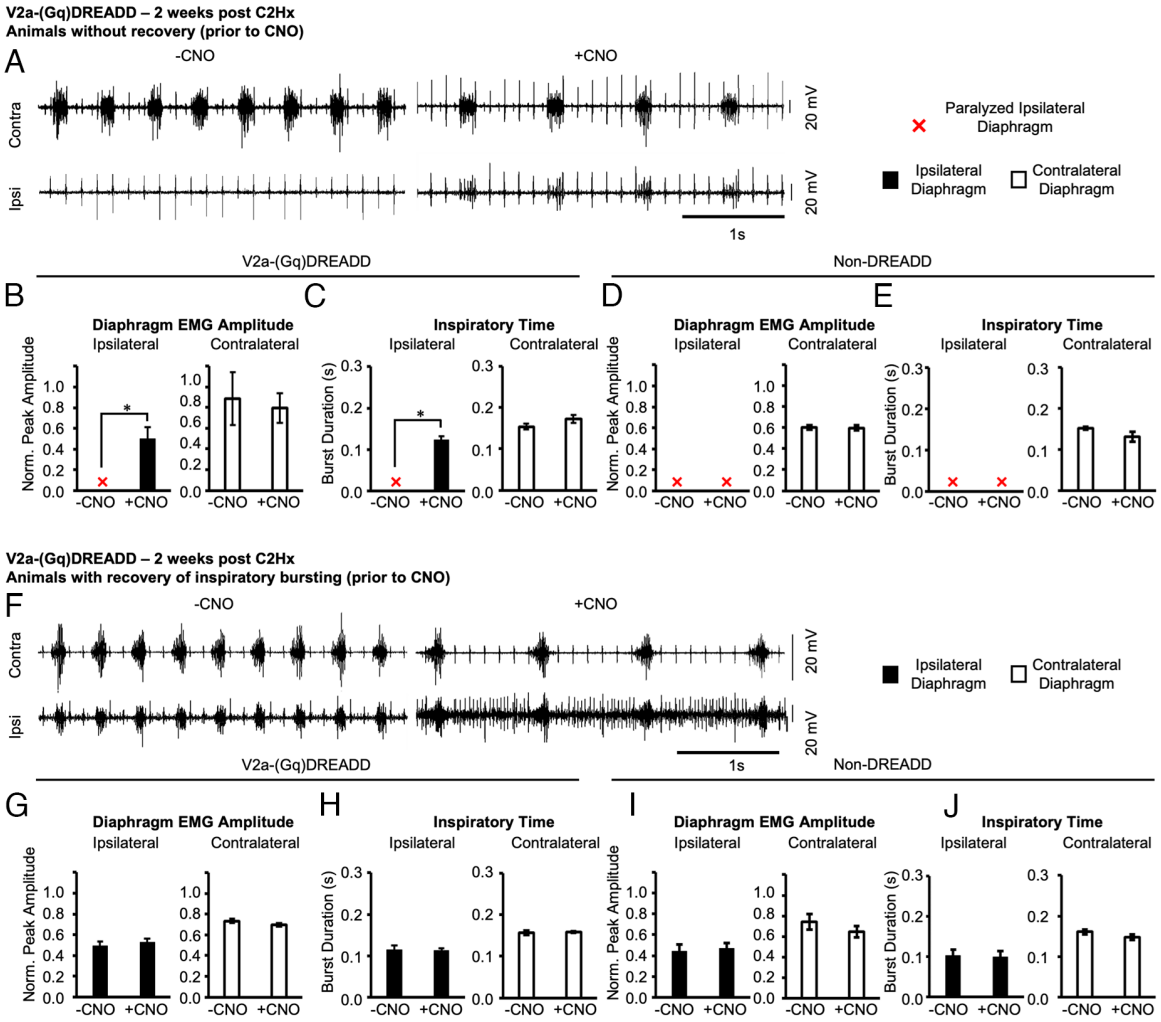

Fig. 3. Increasing the excitability of V2a neurons restores diaphragm function 2 wk following a C2Hx. V2a-(G_q)DREADD mice or non-DREADD-expressing controls received a C2Hx and diaphragm EMG was recorded 2 wk later. (*A*) Representative trace showing the contralateral (*Top*) and ipsilateral (*Bottom*) diaphragm before (*Left*) and after (*Right*) treatment with 1.0 mg/kg*bw CNO in a V2a-(G_q)DREADD animal without recovery (prior to CNO). (*B–E*) The diaphragm EMG peak amplitude (*B* and *D*) and inspiratory time (*C* and *E*) were measured and quantified in V2a-(G_q)DREADD mice and non-DREADD-expressing controls, respectively. (*F*) Representative trace showing the contralateral (*Top*) and ipsilateral (*Bottom*) diaphragm before (*Left*) and after (*Right*) treatment with 1.0 mg/kg*bw CNO in a V2a-(G_q)DREADD animal that showed recovery of inspiratory bursting. (*G–J*) The diaphragm EMG peak amplitude (*G* and *I*) and inspiratory time (*H* and *J*) were measured and quantified in V2a-(G_q)DREADD mice and non-DREADD-expressing controls, respectively. White bars = contralateral diaphragm. Black bars = ipsilateral diaphragm. Red X = paralyzed ipsilateral diaphragm where no bursting activity is detected. The ipsilateral and contralateral diaphragm data were analyzed separately with a parametric paired *t*-test (*C*, *D*, and *G–J*) or non-parametric Wilcoxon signed-rank test (*B* and *E*), $*P < 0.05$.

inspiration is the predominant pattern of diaphragm activity elicited by increasing the excitability of V2a neurons following a C2Hx injury.

In addition to the percent of time spent in each CTA pattern, we also measured the average duration of each CTA pattern before transitioning to a different pattern at each time point following injury. The duration of the rhythmic-only CTA pattern increases as the time following injury increases from 4 h (6.5 ± 4.0 min, n = 3) to 1 d (12.9 ± 10.9 min, n = 9) to 2 wk (25.9 ± 15.9 min, n = 6) post C2Hx ($P < 0.05$) while the average duration of all other CTA patterns decreases, with a significant interaction between the time following the C2Hx and the duration spent in each CTA segment (two-way ANOVA, $P = 0.006$). One day and 2 wk following injury, the rhythmic-only CTA pattern has the greatest duration over any other CTA pattern during that same time point, lasting an average of at least 12 min before transitioning to a different pattern ($P < 0.05$) (Fig. 4*H*). Thus, the rhythmic inspiratory pattern elicited by increasing the excitability of V2a neurons becomes more dominant and stable at the subacute (2 wk) vs. acute (4 h, 1 d) stages after injury.

Silencing V2a Neurons Impairs Chemosensory Stimulated Activation of the Diaphragm Ipsilateral to Injury. We assessed the contribution of V2a neurons for recovery of diaphragm activity 2 wk after a C2Hx by acutely decreasing the excitability of (i.e., "silencing") V2a neurons in 15 V2a-(G_i)DREADD mice. This mouse line expresses the inhibitory (G_i)DREADD and decreases the excitability of V2a neurons in the spinal cord and brainstem following treatment with CNO (30). Two weeks following injury, we measured ipsilateral and contralateral diaphragm EMG to divide mice into three groups (prior to CNO treatment): 1) "non-recovered"- mice with paralyzed ipsilateral diaphragms (n = 5). 2) "recovered- tonic"- mice that show increased ipsilateral diaphragm activity during the expiratory (or both inspiratory and expiratory) phase (n = 3), and 3) "recovered- rhythmic"- mice that show rhythmic inspiratory activity in the ipsilateral diaphragm (n = 7). As in the V2a-(G_q)DREADD experiments, the recovered groups could include animals that spontaneously recovered function as well as animals that were not completely paralyzed at the time of injury. All animals showed lack of chest movement ipsilateral to injury immediately following the C2Hx. There was no difference in the percent of injury observed in the white matter (non-recovered: 38.3 ± 5.4% vs. recovered-tonic: 33.4 ± 1.7% vs. recovered rhythmic: 36.4 ± 6.1%, one-way ANOVA, $P = 0.897$) or gray matter (non-recovered: 32.3 ± 6.5% vs. recovered-tonic: 31.1 ± 1.1% vs. recovered rhythmic: 30.0 ± 4.5%, one-way ANOVA, $P = 0.910$) between the three groups of mice.

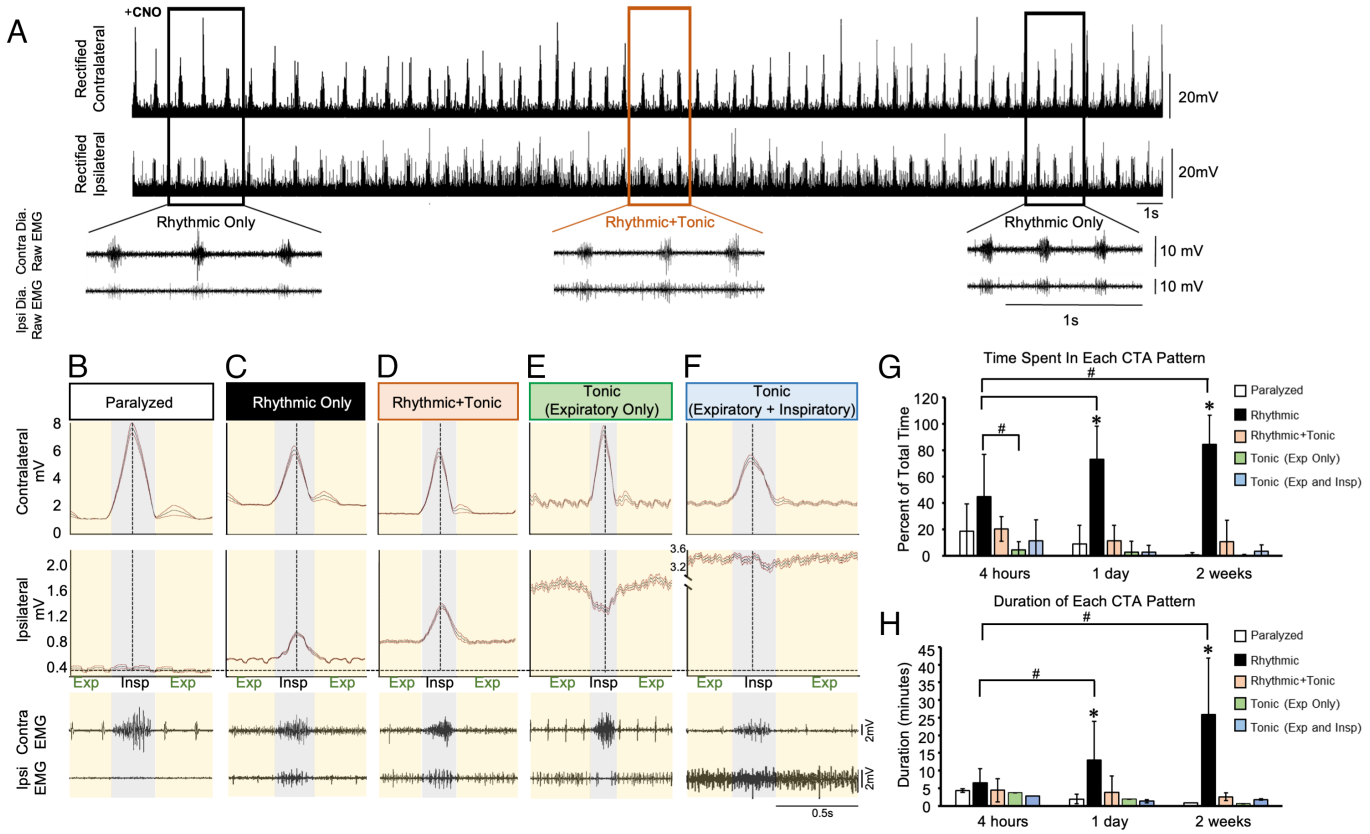

Fig. 4. Cycle triggered averaging reveals that the predominant pattern of diaphragm activity after activating V2a neurons is rhythmic bursting during inspiration. The patterns of diaphragm activity elicited by CNO treatment were analyzed by cycle triggered averaging in V2a-(Gq)DREADD mice 4 h, 1 d, or 2 wk after a C2Hx injury. Only animals without ipsilateral diaphragm activity prior to CNO treatment were included in these analyses. (*A*) Representative ipsilateral and contralateral diaphragm EMG traces from a V2a-(G_q)DREADD mouse 2 wk after a C2Hx and following administration of CNO. The rectified (*Top*) and non-rectified (*Bottom*, from boxed area on top) signals show rhythmic inspiratory activity as well as tonic (throughout the cycle) activity that appears and disappears over time. (*B–F*) Example of cycle triggered averaging (CTA) analysis from the same V2a-(G_q)DREADD animal 1 d following injury to identify and characterize five different patterns of activity. Gray line = average and orange lines = SD for all breaths analyzed during the 20-s period. Inspiration is highlighted in gray while expiration is highlighted in yellow. Example diaphragm EMG traces from the same V2a-(G_q)DREADD animal are shown below the CTA graphs. (*G*) Graph showing the percent of total time that is spent in each CTA pattern following CNO administration in V2a-(G_q) DREADD mice at each time point following the C2Hx injury. (*H*) Graph showing the average duration that is spent in each CTA pattern before transitioning to a different CTA pattern following CNO administration in V2a-(G_q)DREADD mice at each time point following the C2Hx injury. All values shown represent the average ± SD. The number of animals varies by time point: 4 h (n = 3), 1 d (n = 9), and 2 wk (n = 7). White bars = paralyzed CTA pattern. Black bars = rhythmic-only CTA pattern. Orange bars = rhythmic and tonic CTA pattern. Green bars = expiratory only tonic CTA pattern. Blue bars = expiratory and inspiratory tonic CTA pattern. Statistics: *G* and *H* are analyzed with a two-way ANOVA. **P* < 0.05 among the rhythmic-only CTA pattern and all other CTA patterns at that time point post C2Hx. #*P* < 0.05 between the parameters specified by the black bars.

We assessed whether V2a neurons might contribute to activation of the paralyzed diaphragm following maximal chemosensory stimulation, using the non-recovered group of mice (n = 5). We first confirmed that maximal chemosensory stimulation could elicit robust rhythmic inspiratory activity in the diaphragm ipsilateral to injury (Fig. 5 *A* and *B*). The ipsilateral diaphragm returned to a paralyzed state after stimulation ceased. We then silenced V2a neurons by administration of 10.0 mg/kg*bw CNO (30) and repeated the maximal chemosensory stimulation. We measured the diaphragm EMG peak amplitude during stimulation after CNO and expressed it as the percent of diaphragm EMG peak amplitude recorded prior to CNO (from the same side of the diaphragm). CNO treatment reduced diaphragm peak EMG by 59 ± 5% (n = 5, one-way *t*-test, $P < 0.001$) during maximal chemosensory stimulation (Fig. 5*C*). We observed only a 14 ± 10% (n = 5, Student *t* test, $P = 0.007$) change in the contralateral diaphragm peak EMG after CNO treatment. As expected, non-DREADD-expressing control mice (n = 5, $Chx10^{+/+}$; $ROSA^{PNP\text{-}CHRM4/+}$) did not show a difference in ipsilateral (−1.3 ± 21.8%) or contralateral (−6.9 ± 10.8%) diaphragm EMG peak amplitude following 10.0 mg/kg*bw CNO treatment. These results demonstrate that V2a neurons contribute significantly to activation of the paralyzed diaphragm by maximal chemosensory stimulation 2 wk after a C2Hx injury.

Silencing V2a Neurons Impairs Tonic Diaphragm Activity Observed in Animals 2 wk after Injury. We next examined the potential role of V2a neurons in recovery of diaphragm activity under normal breathing conditions (i.e., without maximal chemosensory stimulation). We examined the impact of silencing V2a neurons on the tonic (inspiratory and expiratory) ipsilateral diaphragm activity observed in the recovered-tonic group of V2a-(G_i) DREADD mice (n = 3). Note that we did not observe tonic activity in any animals 4 h or 1 d after injury prior to CNO treatment, suggesting that the tonic activity is a product of spontaneous recovery rather than incomplete injury, consistent with prior studies (55). The tonic activity was abolished in all V2a-(G_i)DREADD mice after silencing V2a neurons with CNO (Fig. 6*A*) indicating that V2a neurons contribute significantly to the tonic activity that is observed during recovery from injury.

We next examined the role of V2a neurons in the recovered-rhythmic group of V2a-(G_i)DREADD mice at 2 wks after injury (n = 7). Silencing V2a neurons drastically reduced the ipsilateral diaphragm EMG peak amplitude by 48.9% in 1/7 V2a-(G_i)DREADD mice (Fig. 6*B*). However, 6/7 animals did not show an appreciable effect of silencing V2a neurons on ipsilateral diaphragm activity. As a group, there was not a significant change in the diaphragm EMG peak amplitude before and after silencing V2a neurons (Ipsi: n = 7, $P = 0.282$; Contra: n = 7, $P = 0.954$) in animals that spontaneously demonstrated recovery of inspiratory burst activity

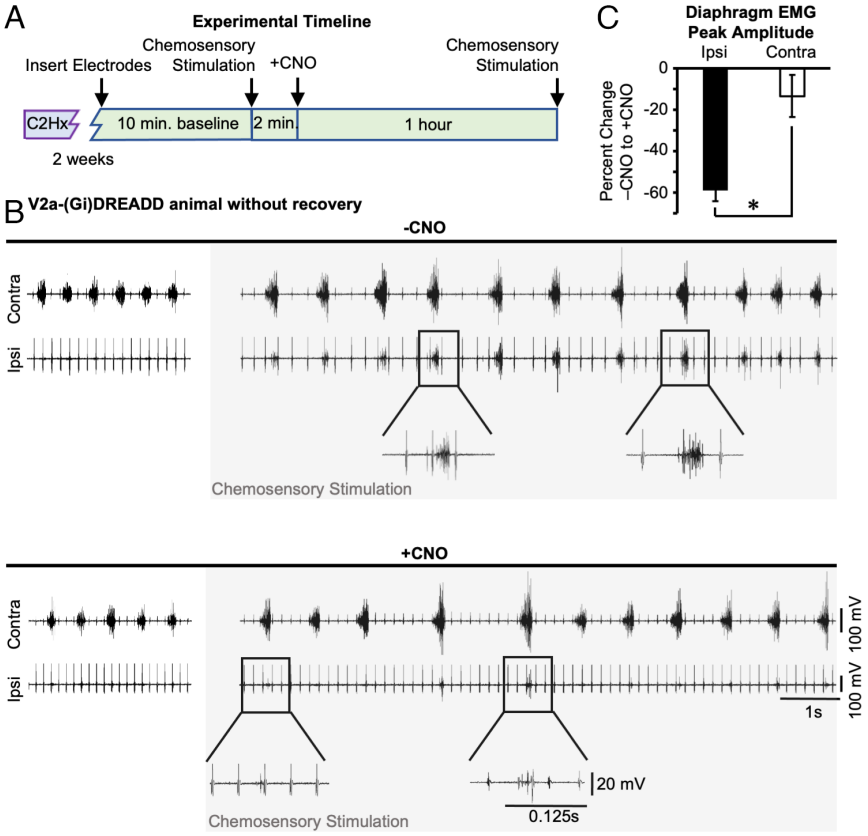

Fig. 5. Silencing V2a neurons after injury impairs chemosensory stimulated activation of the diaphragm. (*A*) Experimental timeline. V2a-(G_i)DREADD mice received a C2Hx and 2 wk later EMG was recorded from the diaphragm contralateral (contra) and ipsilateral (ipsi) to injury. (*B*) Representative traces from an animal without spontaneous recovery of ipsilateral diaphragm activity (*Top*, left). Prior to CNO treatment (−CNO), maximal chemosensory stimulation (gray box) was performed to elicit the crossed phrenic phenomenon. Lower traces are enlarged views of boxed regions, with the same scales used for −CNO (*Top*) and +CNO (*Bottom*) traces. CNO (10.0 mg/kg*bw, +CNO) was administered to decrease the excitability of V2a neurons (+CNO) and maximal chemosensory stimulation (gray box) was once again performed to elicit the crossed phrenic phenomenon after V2a neurons have been silenced. (*C*) The effects of CNO were measured by calculating the percent change (before and after CNO) in diaphragm EMG peak amplitude measured during maximal chemosensory stimulation. White bar = contralateral diaphragm and black bar = ipsilateral diaphragm. Statistics: data (n = 5 mice) were analyzed with a *t*-test, $^*P < 0.05$.

(Fig. 6*D*). We noted that the animal that showed decreased diaphragm activity following CNO treatment had the smallest diaphragm EMG peak amplitude (raw and normalized) of the group prior to CNO treatment. Thus, silencing V2a neurons does not consistently impair robust rhythmic inspiratory activity in the ipsilateral diaphragm 2 wk after a C2Hx injury.

Discussion

Our findings show that the V2a class of excitatory neurons can promote respiratory muscle activity following spinal cord injury. We demonstrate that increasing the excitability of these predominantly ipsilaterally

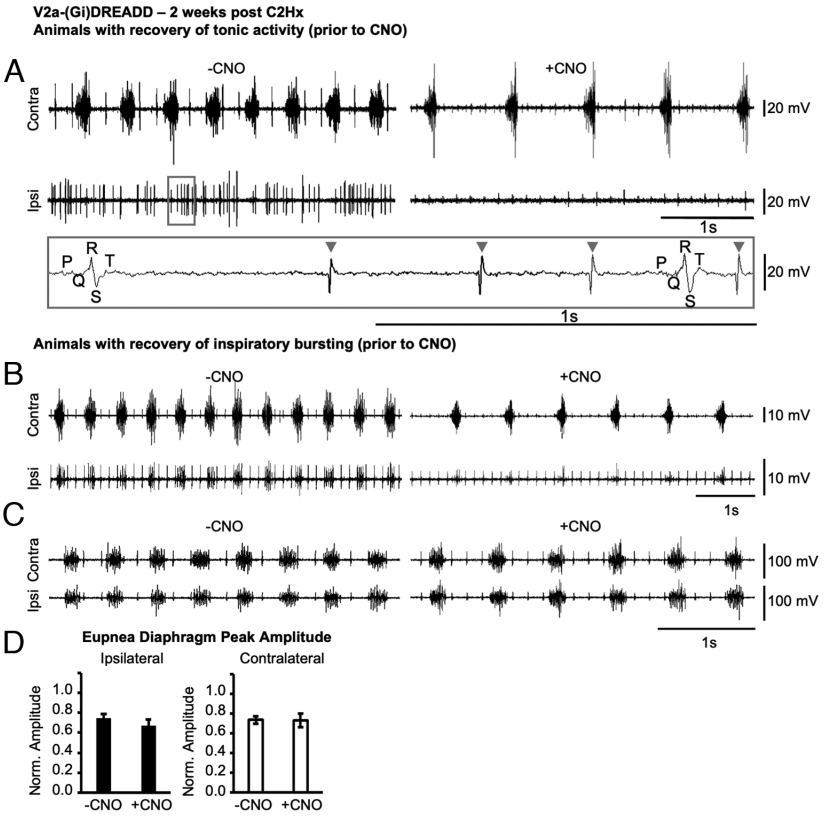

Fig. 6. Silencing V2a neurons inhibits spontaneous tonic diaphragm activity 2 wk following injury. V2a-(G_i)DREADD mice received a C2Hx and 2 wk later EMG was recorded from the diaphragm contralateral (contra) and ipsilateral (ipsi) to injury. (*A*) Representative diaphragm EMG trace from a V2a-(G_i)DREADD animal with spontaneous recovery of tonic activity in the ipsilateral diaphragm prior to CNO treatment (−CNO). Silencing V2a neurons with 10.0 mg/kg*bw CNO (+CNO) abolishes the tonic activity. The gray inset demonstrates that EMG signal (gray arrow heads) is easily distinguished from ECG signal (indicated by PQRST features) at the scale used for analysis. (*B*) Representative diaphragm EMG trace from a V2a-(G_i)DREADD mouse (1/7) that exhibited spontaneous recovery of inspiratory bursting activity and then showed a decrease in EMG peak amplitude following treatment with CNO. (*C*) Representative diaphragm EMG trace from one of the 6/7 V2a-(G_i)DREADD animals that showed spontaneous recovery of inspiratory bursting activity and did not show a decrease in EMG peak amplitude following treatment with CNO. (*D*) Diaphragm EMG peak amplitude from all V2a-(G_i)DREADD animals that showed spontaneous recovery of inspiratory bursting activity is quantified for the ipsilateral (black bar) and contralateral (white bar) diaphragm. Statistics: data (n = 7) were analyzed with a paired *t*-test, $^*P < 0.05$.

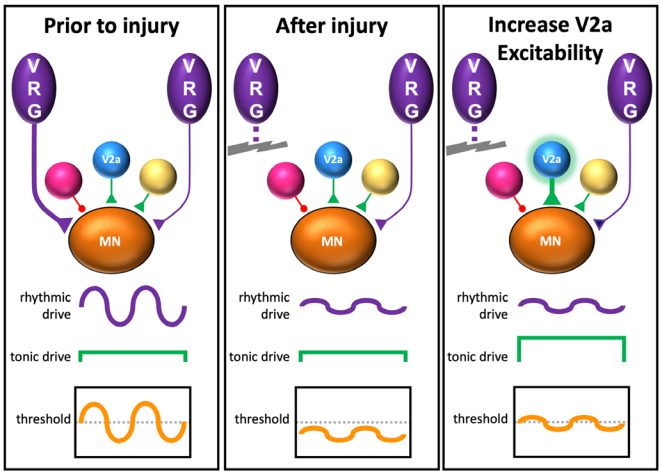

Fig. 7. Hypothetical model of phrenic motor neuron activation by V2a neurons after injury. Prior to injury, phrenic motor neurons (MN) receive strong inputs from the brainstem ventral respiratory group neurons (VRG) whose axons are on the same side of the cord (*Left*) and weak inputs from contralateral VRG neurons and other neurons (red, yellow, and blue "V2a"). The VRG neurons provide rhythmic inspiratory drive that depolarizes motor neurons to their threshold for action potential generation during inspiration. After injury, the weak rhythmic inspiratory drive from spared VRG axons is insufficient to depolarize motor neurons to the threshold for action potential generation, resulting in a paralyzed diaphragm. We propose that increasing the excitability of V2a neurons increases tonic drive to phrenic motor neurons, allowing the weak rhythmic inspiratory drive from the VRG to depolarize motor neurons during inspiration.

projecting excitatory neurons can restore activity to the diaphragm below a C2 hemisection injury without increasing activity of the contralateral diaphragm. In addition, silencing V2a neurons impairs the ability of chemosensory stimulation to activate the diaphragm ipsilateral to injury. Further, silencing V2a neurons prevented tonic diaphragm activity that arose during the recovery period two weeks after injury. Thus, our data support a role for V2a neurons in the circuits that contribute to recovery of respiratory function and suggest that strategies to alter the activity of V2a neurons could improve breathing following injury.

The C2 hemisection model has been an established model to study neural plasticity for over a century (5, 33–38). For example, this model has been used to investigate the "crossed phrenic phenomenon"—the observation that increasing respiratory drive can restore function to a previously paralyzed diaphragm below a C2 hemisection injury via latent pathways from the medulla that cross below the site of injury and directly contact phrenic motor neurons (58, 59). The medullary pre-motor neurons belong to the V0 developmental class of neurons (27), which are distinct from the V2a class. However, a number of studies have indicated that propriospinal neurons also play a role in this phenomenon as well as recovery of breathing after injury (7, 16, 17, 60–64). For example, silencing all glutamatergic neurons in the cervical cord impairs recovery of breathing in the C2 hemisection model, as well as a non-traumatic spinal cord injury model (17). The authors provided evidence that this was via commissural excitatory neurons that may relay respiratory drive from the spared side of the cord to the phrenic motor neurons below the site of injury. Here, we provide evidence that ipsilaterally projecting neurons contribute to or play a permissive role in the crossed phrenic phenomenon (i.e., activation of the previously paralyzed hemidiaphragm following maximal chemosensory drive). Silencing only the V2a subset of neurons [representing less than 1/3 of the excitatory neurons in the ventral spinal cord (65)] significantly reduced activation of the diaphragm ipsilateral to injury following increased chemosensory drive. Although silencing V2a impairs activation of the diaphragm ipsilateral to injury, it has minimal effect on the diaphragm contralateral to injury, whereas targeting both V2a and non-V2a glutamatergic neurons in the cervical cord significantly impairs breathing in injured mice (17).

We hypothesize that V2a neurons provide tonic drive to phrenic motor neurons (or pre-motor neurons) to make them more responsive to spared pathways that provide rhythmic inspiratory drive from the brainstem (Fig. 7). First, increasing the excitability of V2a neurons can induce tonic diaphragm EMG activity (e.g., spikes throughout the respiratory cycle) in both injured and uninjured (30) mice. Second, silencing V2a neurons eliminates tonic activity that spontaneously occurs in mice 2 wk after spinal cord injury but is not observed 4 h or 1 d after injury. Previous studies in rats measuring phrenic motor neuron discharge patterns following a C2 hemisection demonstrated the emergence of tonically firing motor neurons 2 wk (and persisting for at least 8 wk) after injury (55). It was proposed that this tonic activity was the result of spontaneous plastic changes in respiratory circuits, which likely include changes in intrinsic motor neuron properties and/or formation of new synaptic inputs to motor neurons after injury. Tonic phrenic activity can also be elicited by optogenetically exciting spinal circuits 4 d after injury (66), indicating that it can be driven at the spinal level. The observation that increased connectivity between cervical V2a neurons and phrenic motor neurons (31) and the emergence of tonic activity both occur within 2 wk after injury is also consistent with the idea that increased connectivity between V2a (and possibly other) spinal neurons increases tonic drive to phrenic motor neurons, thereby allowing them to respond to weak inspiratory drive provided by spared pathways. Importantly, our results do not rule out a role for V2a neurons in directly relaying rhythmic inspiratory drive to phrenic motor neurons and it is even possible that V2a neurons could provide both tonic and rhythmic drive. For example, in the lumbar cord, some V2a neurons are rhythmically active during fictive locomotion whereas other V2a neurons fire tonically (67, 68). Since our studies targeted both spinal and brainstem V2a, we cannot rule out the possibility that brainstem V2a contribute to activation of the diaphragm after injury. This could occur via spared reticulospinal projections or projections to brainstem respiratory neurons. The lack of a significant effect of increasing the excitability of V2a on the activity of the diaphragm contralateral to injury argues against a role for V2a in increasing respiratory drive at the level of the brainstem, but does not disprove this possibility.

After increasing the excitability of V2a neurons, animals show spontaneous changes in the pattern of diaphragm activity ipsilateral to injury over time (rhythmic inspiratory, tonic, or a combination of rhythmic + tonic). However, the reason(s) for these changes in pattern are not currently clear. Movement or changes in posture are not possible since the animals are anesthetized and immobile. We also see no evidence for changes in the depth of anesthesia during breathing transitions. The animals are freely breathing, so it is possible that fluctuations in blood oxygen or carbon dioxide trigger changes in the motor pattern. Prior studies showed that increasing respiratory drive (by increasing end-tidal CO_2) could increase the probability that phrenic motor neurons below a C2Hx lesion would fire during inspiration as opposed to tonically (55). This result is consistent with a model in which both tonic and phasic inputs drive phrenic motor neuron output. Alternatively, fluctuations in neurotransmitter release may drive changes in motor patterns. For example, our previous study showed that tonic activity (or a combination of rhythmic and tonic activity) is observed in the ipsilateral diaphragm of C2 hemisectioned rats following treatment with serotonin or treatments that altered serotonergic innervation of the spinal cord (69). Future experiments should investigate potential interactions between V2a neurons and serotonergic neurons in the control of phrenic motor neuron output. Although efficient breathing likely requires predominantly inspiratory bursting activity, tonic activity may represent an early stage of recovery. If true, our data would suggest that therapies targeting V2a neurons would be most beneficial during early stages or severe injuries but would likely be less effective if robust inspiratory activity has already been achieved.

We found an increase in the proportion and duration of rhythmic activity caused by activating V2a neurons at 2 wk compared to 1 d after injury, despite evidence that new V2a neurons are recruited into phrenic circuitry 2 wk following injury (31). If non-respiratory neurons were recruited into respiratory circuits, one might predict more tonic rather than rhythmic activity. One explanation is that the increase in connectivity to phrenic motor neurons from V2a neurons is accompanied by an increase in connectivity (or strength of connections) from spared brainstem pathways. Changes in the intrinsic properties of motor neurons or neuromodulatory input (e.g., serotonin) over the subacute period may also play a role. Importantly, although the ipsilateral diaphragm is paralyzed prior to CNO treatment in our experiments, we cannot rule out the possibility that

activity-dependent plasticity plays a role in rhythmic versus tonic firing patterns. This is because our diaphragm EMG recordings are made under anesthesia [known to inhibit recovery of diaphragm function (43)], and it is possible that there is some activity in ipsilateral phrenic motor neurons during the 2 wk following injury while the animal is not under anesthesia. Future studies will need to investigate the potential of V2a neurons to restore diaphragm function in cases of chronic injury since our studies did not assess the impact of increasing V2a neuron excitability beyond 2 wk of age or evaluate the effects of chronically altering V2a neuron excitability.

Importantly, restoring activity to phrenic motor neurons by targeting V2a neurons does not require formation of de novo circuits, because increasing the excitability of V2a neurons can restore diaphragm function as early as 4 h after injury and produce tonic activity in uninjured animals. Thus, V2a neurons likely contribute to control of diaphragm activity in healthy animals, although their role is currently not defined. Since V2a neurons are not required for normal breathing in adult mice at rest (30), these neurons may only be needed under certain conditions, such as behaviors with high ventilatory demands like running or non-ventilatory behaviors such as coughing or vocalizing (29, 53, 70). To better understand the role of V2a neurons in healthy animals, additional studies are necessary to measure and/or alter the activity of V2a neurons during different behaviors and assess their role in breathing.

Our data provide evidence suggesting that V2a neurons would be strong candidates to target therapeutically to improve breathing after injury. First, despite numerous long propriospinal and supraspinal connections, we detected no significant loss of V2a neurons or axons below a hemisection injury, indicating that V2a are resilient. Second, altering V2a activity appears relatively safe without known adverse effects on motor behaviors. For example, activating V2a neurons is unlikely to impact brainstem control of breathing (e.g., chemosensation) because V2a neurons appear to increase activity of the diaphragm without increasing respiratory drive. This data is consistent with our prior studies showing that altering the activity of V2a neurons does not impair breathing in healthy adult mice, despite the fact that V2a neurons provide excitatory drive to brainstem rhythm generating neurons necessary for regular breathing rhythm during the neonatal period (29, 30, 65, 71). Further, activating V2a neurons does not appear to adversely affect other motor functions, like walking (22, 29, 30, 71). Future experiments to identify druggable molecules expressed by V2a neurons and/or develop improved methods (e.g., electrical stimulation) to target these neurons in humans could lead to advances in the treatment of respiratory insufficiency following spinal cord injury.

Materials and Methods

Animal Models to Label or Alter Excitability of V2a Neurons. V2a-(G_q)DREADD mice ($Chx10^{Cre/+}$; $ROSA^{PNP\text{-}tTA/+}$; $Tg^{TetO\text{-}CHRM3/+}$) (JAX# 008600; JAX# 014093) express the G_q excitatory DREADD receptor in brainstem and spinal cord V2a neurons, as well as the eye (29). In these mice, the endogenous Chx10 regulatory region drives expression of Cre recombinase, which removes a loxP flanked stop sequence and allows expression of the tetracycline controlled transactivator (tTA) in $Chx10^{+}$ V2a neurons. Binding of the tetracycline controlled transactivator (tTA) to the Tet operator (TetO) drives (G_q)DREADD expression in V2a neurons. Doxycycline, which blocks tTA activity, was not administered to any animals. Treatment of V2a-(G_q)DREADD mice with clozapine-N-oxide (**CNO**) activates G_q signaling in V2a neurons, increasing their excitability, as previously described (29). Non-DREADD-expressing controls include both ($Chx10^{Cre/+}$; $ROSA^{PNP\text{-}tTA/+}$; $Tg^{+/+}$) and ($Chx10^{+/+}$; $ROSA^{PNP\text{-}tTA/+}$; $Tg^{TetO\text{-}CHRM3/+}$) mice.

V2a-(G_i)DREADD mice ($Chx10^{Cre/+}$; $ROSA^{PNP\text{-}CHRM4/+}$) (JAX# 026219) express the (G_i) inhibitory DREADD receptor in brainstem and spinal cord V2a neurons, as well as the eye. Treatment with CNO acutely decreases the excitability of V2a neurons, as previously described (30). CNO was delivered by topical application to the exposed intraperitoneal cavity in all experiments. Our prior studies demonstrated that higher doses of CNO are required to silence neurons in V2a-(G_i)DREADD mice (10.0 mg/kg*bw CNO) (30) than are required to increase the excitability of V2a neurons in V2a-(G_q)DREADD mice (1.0 mg/kg*bw CNO) (29), consistent with other reports (72).

Although rare, we occasionally observe widespread expression of DREADDs (or other reporters) in $Chx10^{Cre/+}$ animals, likely due to sporadic expression of Cre recombinase in the germline or early embryo. We used PCR to detect abnormal recombination in tail DNA from V2a-(G_i)DREADD animals as previously described (30) and eliminated these animals from our experiments. In order to eliminate V2a-(G_q)DREADD mice with abnormal recombination, we performed immunohistochemistry on tail tissue using an antibody that recognizes the HA-tag on the (G_q)DREADD (rabbit anti-HA at 1:1000, Cell Signaling #3724).

Spinal Cord Tissue Clearing. The spinal column, including the spinal cord, lower brainstem, spine, and surrounding muscle, was harvested from V2a-tdTomato mice after perfusion with phosphate buffered saline solution followed by 4% paraformaldehyde in phosphate buffer (PFA). Columns were post-fixed overnight in PFA at 4 °C. The spinal cords were dissected out, meninges removed, and the tissue was optically cleared using a modified version of the passive CLARITY technique (PACT) as previously described (73). Briefly, spinal cords were cross-linked with an acrylamide hydrogel solution containing VA-044 thermal initiator and then delipidated over the course of 6 d in a clearing solution consisting of 8% SDS in 0.2 M boric acid buffer. Following clearing, samples were immunolabeled with anti-ChAT antibody (1:500; MilliporeSigma) and AlexaFluor Plus 647 secondary antibody (1:500, Thermo Fisher). After staining and washing, samples were mounted in 1.5% agarose in 1 mL syringes and equilibrated in refractive index matching solution (RIMS) for 2 d.

3D Lightsheet Imaging and Image Analysis. Cleared spinal cord samples were imaged on a Zeiss Z1 lightsheet microscope with a 5×/0.16 NA objective. Multiple images spanning the length of the cervical region of the spinal cord were acquired and stitched together using Imaris Stitcher software (BitPlane) or the FIJI BigStitcher plugin. The image Z-stacks were imported into Imaris software and V2a interneuron soma were counted using the built-in spots feature and the in-app machine learning toolkit. Manual neurite counting along the spinal cord midline at C5 was performed in Image J by two independent observers. Image data were analyzed using Prism software (GraphPad).

Fluorescence-based Tractography. Tractography was performed in MATLAB using code modified from Ye et al. 2016. Briefly, the lightsheet images were convolved with a derivative of the Gaussian kernel to compute the gradients of fluorescent intensity within a local neighborhood of each voxel. A structure tensor matrix was computed for each voxel from the image intensity gradients. Structure tensor matrices were converted to .nii files and input into Diffusion Toolkit software (TrackVis) to derive the tertiary eigenvector at each voxel. The resulting eigenvectors, along with image thresholds and manually designated seed regions, were used to create streamlines following V2a neuron axon tracts in the lightsheet images. TrackVis software (TrackVis) was then used to display and quantify the streamlines.

C2Hx Spinal Cord Injury Surgeries. Lesions to one half of the spinal cord at C2 (C2Hx) were performed in adult mice (age 73 to 145 d, males and females) under isoflurane anesthesia. Blunt dissection of the paravertebral muscles using cotton tip applicators exposed the back of the skull and the cervical vertebrae. Microscissors were used to perform a laminectomy. Once the spinal cord was exposed, a 30G needle was used to hemisect the left side of the spinal cord just caudal to the C2 dorsal root. Multiple needle passes (up to 5) were performed until a complete injury was confirmed by observing the lack of chest wall movement on the side of the injury (but normal breathing movements on the contralateral side). The paravertebral muscles were sutured back together following the C2Hx. Dermal adhesive was used to close the skin incision. Immediately following the surgery, mice were injected subcutaneously with carprofen (5mg/kg*BW) and placed in an incubator set at 29 °C overnight. Each cage was supplied with nutritional gel and a water bottle. Mice also received subcutaneous injections of 1.0 mL saline twice daily for the first two post-operative care days following surgery.

Terminal Bilateral Diaphragm EMG Recordings. Terminal bilateral diaphragm EMG recordings were performed in separate cohorts of animals at the following time points: 4 h, 1 d, or 15 d (i.e., 2 wk) after the C2Hx surgery, or in uninjured control mice. Animals were anesthetized under 1% isoflurane/1% oxygen and placed supine on a heating pad. A 4-cm lateral incision through the skin and abdominal muscle just below the xiphoid process exposed the intraperitoneal cavity and diaphragm. Bipolar electrodes connected to an amplifier (BMA-400 AC/DC Bioamplifier) were inserted into both hemidiaphragms (left and right) to record diaphragmatic activity via Spike2 Data Analysis software (Cambridge

Electronic Design Limited, Cambridge, England). Electrodes were grounded with an additional lead inserted into the abdominal muscle.

A 10-min baseline of bilateral diaphragm activity was recorded. Animals with incomplete C2Hx injury (e.g., they did not show complete paralysis of the hemidiaphragm below the C2Hx lesion) at acute (4 h or 1 d) time points were excluded from further analysis (1/10 V2a-(G_q)DREADD mice, 2/9 non-DREADD-expressing controls at 1-d time point, 2/9 V2a-(G_q)DREADD mice at 4 h time point). CNO was then topically applied to the exposed intraperitoneal cavity and the effect on diaphragm EMG was recorded for 60 min. We induced maximal chemosensory stimulation (70) by performing three 15-s nasal occlusions, each separated by a 10-s break. All animals at 1 d or 2 wk following injury responded to chemosensory stimulation with rhythmic inspiratory bursting in the previously paralyzed diaphragm. At the 4 h post injury time point, we excluded animals that did not exhibit rhythmic bursting activity following chemosensory stimulation (4/7 animals), a ratio consistent with previous studies performed within hours after injury (74). Diaphragm activity was allowed to return to the pre-stimulated level before stopping the recording, removing the electrodes, and harvesting the brain and spinal cord. All mice were maintained at 1% isoflurane/1% oxygen for the entire recording.

Assessing the Extent of Anatomical Damage Due to the C2Hx injury. The harvested brains and spinal cords were placed in 4%PFA in 10× PB for 24 h. The tissue was then transferred into 1× PBS and washed on a rocker O/N before being placed in cryoprotectant 30% sucrose O/N. Cervical segments 1–6 were embedded in OCT compound and stored at −80C until sectioned. Cervical tissue was sectioned at 20 μM thickness using a cryostat. Every third section was stained with cresyl violet to measure spared spinal cord tissue (54). Briefly, sectioned spinal cord tissue was dehydrated, placed in xylenes and rehydrated before staining in cresyl violet for 6 min. Tissue was then dehydrated again, placed in xylenes and coverslipped with permount. This cervical tissue was then imaged with the Zeiss Axio Scan.Z1 at C2 to assess the completeness and consistency of the C2Hx lesions. The spinal cord section with the greatest amount of damage was assessed for the extent of injury for each animal as previously described (54). Briefly, ImageJ was used to trace the outline and measure the area of the spared gray matter and spared white matter. The total area of the spinal cord was estimated by multiplying the area of the gray matter or white matter in the uninjured half of the spinal cord by 2. The percent of injury out of the total area of the spinal cord was separately calculated for the gray and white matter using the following equation:

$$\%\,\text{injury} = [(2 \times \text{HemicordArea}) - (\text{TotalSparedTissueArea})]/(2 \times \text{HemicordArea}) \times 100$$

Diaphragm EMG Analysis. The diaphragm EMG signal was amplified (gain 2,000×) and bandpass filtered (30 to 3,000 Hz) with a sampling frequency of 6.25 kHz. EMG signals were further processed to remove DC noise and subsequently rectified and integrated over a 50 ms window. Electrocardiogram (ECG) artifact was digitally filtered out using the "ECGDelete02" Spike2 script (Cambridge Electronic Design) in traces where the ECG amplitude exceeded the diaphragm EMG amplitude. ECG was distinguished from EMG activity by its regular occurrence (~9 to 11 Hz) and its characteristic shape with definitive QRST peaks (75). The rectified and integrated signal was used to calculate the raw EMG peak amplitude for at least 30 s before and after CNO treatment. These values were normalized to the raw EMG peak amplitude recorded during maximum ventilatory effort (nasal occlusion) in order to reduce intra-animal variability (53). Respiratory cycle and inspiratory time were also analyzed for each breath using the rectified and integrated signal from the same time period analyzed for peak amplitude. The regularity of breathing was assessed by calculating the coefficient of variation of bursting frequency (CV_f). CV_f for each animal reflects the average value over each 30-s analysis period.

Cycle Triggered Averaging. We performed cycle triggered averaging (CTA) on rectified and integrated diaphragm EMG signals to correlate the phase of the respiratory cycle (inspiration vs. expiration) from the ipsilateral diaphragm with that seen in the intact contralateral diaphragm. The rectified and integrated EMG signal from the intact contralateral diaphragm was used as a reference to define inspiration vs. expiration. Spike2 was used to generate a memory channel that marked the onset of expiration (channel m1) in the contralateral diaphragm based on the falling threshold amplitude detected from the processed contralateral diaphragm channel for each period of analysis. Next, an average waveform for all breaths in a 20-s analysis period was generated for the contralateral and ipsilateral processed diaphragm channel. Each waveform was generated using the previously generated contralateral memory channel (m1) as the reference channel. The offset value was specified as 0.5 s while the width was set to the maximum respiratory period in each period of analysis in order to encompass the entire respiratory cycle. Each waveform generated reflects the average and SD for all breaths analyzed within the 20-s analysis period. The final waveform graphs highlight the inspiratory and expiratory periods. The inspiratory period was defined as the average duration of the inspiratory time during the analyzed period prior to the onset of expiration in the contralateral diaphragm channel.

Statistical Analysis. Diaphragm EMG peak amplitude and inspiratory time for the ipsilateral and contralateral diaphragm before and after CNO treatment were analyzed with separate paired *t*-tests. Data that failed the normality test were analyzed with the Wilcoxon signed rank test (indicated in figure legend when applicable). The CV_f between the ipsilateral and contralateral diaphragm under one condition only were compared using Student *t*-tests (i.e., CV_f between the ipsilateral and contralateral diaphragm post CNO). Data that failed the normality test were analyzed with the non-parametric equivalent Mann–Whitney U-test instead (indicated in figure legend when applicable). Analysis of frequency changes over time ("run-down" experiment) was performed via mixed effects model (REML) using repeated measures with Tukey post-hoc analysis. A one-way ANOVA was used to compare the average amount of time it took for CNO to produce a response from the ipsilateral diaphragm in V2a-(G_q)DREADD mice among the different time points: 4 h, 1 d, and 2 wk post C2Hx. A two-way ANOVA was used to compare the percentage of time spent in each cycle triggered average pattern among the different time points following the C2Hx spinal cord injury. Chi-square tests of independence were used to analyze how the presence of the (G_q)DREADD receptor in V2a neurons were related to two mutually exclusive outcomes (i.e., tonic activity vs. no tonic activity). When the expected outcome from a chi-square test was less than 5, a Fisher's exact test was used to accurately analyze a 2 × 2 contingency table with small sample sizes. Data are reported as average ± SEM. The significance level is set at $P = 0.05$ with (*) a two-tailed $P < 0.05$.

Data, Materials, and Software Availability. All study data are included in the main text.

ACKNOWLEDGMENTS. We would like to thank Daimen R. S. Britsch and Lydia E. Strattan for developing the technique to record electromyography from the mouse diaphragm. Some of the material in this manuscript was used in the doctoral dissertation of Victoria Jensen. This publication was supported by a collaborative grant to S.A.C. and W.J.A. from the National Center for Research Resources and the National Center for Advancing Translational Sciences, NIH, through Grant UL1TR001998, the University of Kentucky College of Medicine, and Office of the Vice President for Research as well as by the CCTST at the University of Cincinnati-funded by the NIH Clinical and Translational Science Award (CTSA) program, Grant 5UL1TR001425-03. The CTSA program is led by the NIH's National Center for Advancing Translational Sciences (NCATS). Additional support was provided by Craig H. Neilsen Foundation Grants #598928 (S.A.C.) and #598741 (W.J.A.), Cincinnati Children's Hospital Medical Center Research and Innovation Pilot Grant (S.A.C.), the L.B. Research and Education Foundation (I.W.), Mission Connect- a program of TIRR Foundation (D.A.M.), Silicon Valley Community Foundation CZI Imaging Scientist Program 2019-198168 (H.C.G.) as well as the NIH R01NS112255 (S.A.C.), R01NS101105 (W.J.A.), and R01NS122961 (D.A.M.). The content is solely the responsibility of the authors and does not necessarily represent the official views of the NIH or other funding agencies.

Author affiliations: [a]Neuroscience Graduate Program, University of Cincinnati College of Medicine, Cincinnati, OH 45219; [b]Department of Neuroscience, University of Kentucky College of Medicine, Lexington, KY 40536; [c]Spinal Cord and Brain Injury Research Center, University of Kentucky College of Medicine, Lexington, KY 40536; [d]Department of Biology, Texas A&M University, College Station, TX 77843; [e]Department of Biomedical Engineering, Texas A&M University, College Station, TX 77843; [f]Division of Neurosurgery, Cincinnati Children's Hospital Medical Center, Cincinnati, OH 45229; [g]Medical Scientist Training Program, University of Cincinnati College of Medicine, Cincinnati, OH 45267; [h]Microscopy and Imaging Center, Texas A&M University, College Station, TX 77843; [i]Texas A&M Institute for Neuroscience, Texas A&M University, College Station, TX 77843; [j]Division of Developmental Biology, Cincinnati Children's Hospital Medical Center, Cincinnati, OH 45229; and [k]Department of Neurosurgery, University of Cincinnati College of Medicine, Cincinnati, OH 45267

1. M. Berlly, K. Shem, Respiratory management during the first five days after spinal cord injury. *J. Spinal Cord. Med.* **30**, 309–318 (2007).
2. D. J. Berlowitz, B. Wadsworth, J. Ross, Respiratory problems and management in people with spinal cord injury. *Breathe (Sheff)* **12**, 328–340 (2016).
3. L. D. Hachem, C. S. Ahuja, M. G. Fehlings, Assessment and management of acute spinal cord injury: From point of injury to rehabilitation. *J. Spinal Cord. Med.* **40**, 665–675 (2017).
4. R. A. Johnson, G. S. Mitchell, Common mechanisms of compensatory respiratory plasticity in spinal neurological disorders. *Respir. Physiol. Neurobiol.* **189**, 419–428 (2013).
5. P. M. Warren, W. J. Alilain, The challenges of respiratory motor system recovery following cervical spinal cord injury. *Prog. Brain Res.* **212**, 173–220 (2014).
6. K. M. Hormigo *et al.*, Enhancing neural activity to drive respiratory plasticity following cervical spinal cord injury. *Exp. Neurol.* **287**, 276–287 (2017).
7. V. N. Jensen, W. J. Alilain, S. A. Crone, Role of propriospinal neurons in control of respiratory muscles and recovery of breathing following injury. *Front. Syst. Neurosci.* **13**, 84 (2019).
8. M. L. Randelman, L. V. Zholudeva, S. A. Crone, M. A. Lane, "Spinal interneurons and breathing" in *Spinal Interneurons: Plasticity after Spinal Cord Injury*, L. V. Zholudeva, M. A. Lane, Eds. (Elesevier, 2023), chap. 9, pp. 251–275, 10.1016/b978-0-12-819260-3.00014-7.
9. F. M. Bareyre *et al.*, The injured spinal cord spontaneously forms a new intraspinal circuit in adult rats. *Nat. Neurosci.* **7**, 269–277 (2004).
10. O. Raineteau, K. Fouad, F. M. Bareyre, M. E. Schwab, Reorganization of descending motor tracts in the rat spinal cord. *Eur. J. Neurosci.* **16**, 1761–1771 (2002).
11. G. Courtine *et al.*, Recovery of supraspinal control of stepping via indirect propriospinal relay connections after spinal cord injury. *Nat. Med.* **14**, 69–74 (2008).
12. L. Filli, M. E. Schwab, Structural and functional reorganization of propriospinal connections promotes functional recovery after spinal cord injury. *Neural. Regen. Res.* **10**, 509–513 (2015).
13. J. R. Flynn, B. A. Graham, M. P. Galea, R. J. Callister, The role of propriospinal interneurons in recovery from spinal cord injury. *Neuropharmacology* **60**, 809–822 (2011).
14. T. Bezdudnaya, V. Marchenko, L. V. Zholudeva, V. M. Spruance, M. A. Lane, Supraspinal respiratory plasticity following acute cervical spinal cord injury. *Exp. Neurol.* **293**, 181–189 (2017).
15. S. Vinit, A. Kastner, Descending bulbospinal pathways and recovery of respiratory motor function following spinal cord injury. *Respir. Physiol. Neurobiol.* **169**, 115–122 (2009).
16. K. A. Streeter *et al.*, Mid-cervical interneuron networks following high cervical spinal cord injury. *Respir Physiol. Neurobiol.* **271**, 103305 (2020).
17. K. Satkunendrarajah, S. K. Karadimas, A. M. Laliberte, G. Montandon, M. G. Fehlings, Cervical excitatory neurons sustain breathing after spinal cord injury. *Nature* **562**, 419–422 (2018).
18. S. Grillner, A. El Manira, Current principles of motor control, with special reference to vertebrate locomotion. *Physiol. Rev.* **100**, 271–320 (2020).
19. M. Sengupta, M. W. Bagnall, Spinal interneurons: Diversity and connectivity in motor control. *Annu. Rev. Neurosci.* **46**, 79–99 (2023), 10.1146/annurev-neuro-083122-025325.
20. A. C. Wilson, L. B. Sweeney, Spinal cords: Symphonies of interneurons across species. *Front. Neural. Circuits* **17**, 1146449 (2023).
21. R. Vavrek, D. D. Pearse, K. Fouad, Neuronal populations capable of regeneration following a combined treatment in rats with spinal cord transection. *J. Neurotrauma* **24**, 1667–1673 (2007).
22. C. Kathe *et al.*, The neurons that restore walking after paralysis. *Nature* **611**, 540–547 (2022).
23. D. C. Lu, T. Niu, W. A. Alaynick, Molecular and cellular development of spinal cord locomotor circuitry. *Front. Mol. Neurosci.* **8**, 25 (2015).
24. C. Y. Peng *et al.*, Notch and MAML signaling drives Scl-dependent interneuron diversity in the spinal cord. *Neuron* **53**, 813–827 (2007).
25. Y. M. Clovis *et al.*, Chx10 consolidates V2a interneuron identity through two distinct gene repression modes. *Cell Rep.* **16**, 1642–1652 (2016).
26. P. A. Gray, Transcription factors and the genetic organization of brain stem respiratory neurons. *J. Appl. Physiol.* **104**, 1513–1521 (2008).
27. J. Wu *et al.*, A V0 core neuronal circuit for inspiration. *Nat. Commun.* **8**, 544 (2017).
28. S. A. Crone *et al.*, Genetic ablation of V2a ipsilateral interneurons disrupts left-right locomotor coordination in mammalian spinal cord. *Neuron* **60**, 70–83 (2008).
29. S. H. Romer *et al.*, Accessory respiratory muscles enhance ventilation in ALS model mice and are activated by excitatory V2a neurons. *Exp. Neurol.* **287**, 192–204 (2017).
30. V. N. Jensen, K. Seedle, S. M. Turner, J. N. Lorenz, S. A. Crone, V2a neurons constrain extradiaphragmatic respiratory muscle activity at rest. *eNeuro* **6**, ENEURO.0492-18.2019 (2019).
31. L. V. Zholudeva, J. S. Karliner, K. J. Dougherty, M. A. Lane, Anatomical recruitment of spinal V2a interneurons into phrenic motor circuitry after high cervical spinal cord injury. *J. Neurotrauma* **34**, 3058–3065 (2017).
32. L. V. Zholudeva *et al.*, Transplantation of neural progenitors and V2a interneurons after spinal cord injury. *J. Neurotrauma* **35**, 2883–2903 (2018), 10.1089/neu.2017.5439.
33. M. G. Z. Ghali, The crossed phrenic phenomenon. *Neural Regen. Res.* **12**, 845–864 (2017).
34. H. G. Goshgarian, The crossed phrenic phenomenon and recovery of function following spinal cord injury. *Respir. Physiol. Neurobiol.* **169**, 85–93 (2009).
35. H. G. Goshgarian, The crossed phrenic phenomenon: A model for plasticity in the respiratory pathways following spinal cord injury. *J. Appl. Physiol.* **94**, 795–810 (2003).
36. W. T. Porter, The path of the respiratory impulse from the bulb to the phrenic nuclei. *J. Physiol.* **17**, 455–485 (1895).
37. O. Langendorff, Ueber die Folgen einer halbseitigen Abstragung des Kopfmarkes. *Archiv. Fur. Physiol.*, 289–295 (1887).
38. L. J. Lewis, J. M. Brookhart, Significance of the crossed phrenic phenomenon. *Am. J. Physiol.* **166**, 241–254 (1951).
39. K. D. Nantwi, H. G. Goshgarian, Adenosinergic mechanisms underlying recovery of diaphragm motor function following upper cervical spinal cord injury: Potential therapeutic implications. *Neurol. Res.* **27**, 195–205 (2005).
40. V. Hernandez-Torres *et al.*, BDNF effects on functional recovery across motor behaviors after cervical spinal cord injury. *J. Neurophysiol.* **117**, 537–544 (2017).
41. W. J. Alilain, K. P. Horn, H. Hu, T. E. Dick, J. Silver, Functional regeneration of respiratory pathways after spinal cord injury. *Nature* **475**, 196–200 (2011).
42. B. J. Dougherty, K. Z. Lee, M. A. Lane, P. J. Reier, D. D. Fuller, Contribution of the spontaneous crossed-phrenic phenomenon to inspiratory tidal volume in spontaneously breathing rats. *J. Appl. Physiol.* **112**, 96–105 (2012).
43. T. Bezdudnaya, K. M. Hormigo, V. Marchenko, M. A. Lane, Spontaneous respiratory plasticity following unilateral high cervical spinal cord injury in behaving rats. *Exp. Neurol.* **305**, 56–65 (2018).
44. S. Vinit *et al.*, Long-term reorganization of respiratory pathways after partial cervical spinal cord injury. *Eur. J. Neurosci.* **27**, 897–908 (2008).
45. M. B. Zimmer, K. Nantwi, H. G. Goshgarian, Effect of spinal cord injury on the respiratory system: Basic research and current clinical treatment options. *J. Spinal. Cord Med.* **30**, 319–330 (2007).
46. D. J. Hoh, L. M. Mercier, S. P. Hussey, M. A. Lane, Respiration following spinal cord injury: Evidence for human neuroplasticity. *Respir Physiol. Neurobiol.* **189**, 450–464 (2013).
47. D. J. Urban, B. L. Roth, DREADDs (designer receptors exclusively activated by designer drugs): Chemogenetic tools with therapeutic utility. *Annu. Rev. Pharmacol. Toxicol.* **55**, 399–417 (2015).
48. H. M. Lee, P. M. Giguere, B. L. Roth, DREADDs: Novel tools for drug discovery and development. *Drug Discovery Today* **19**, 469–473 (2014).
49. E. Azim, J. Jiang, B. Alstermark, T. M. Jessell, Skilled reaching relies on a V2a propriospinal internal copy circuit. *Nature* **508**, 357–363 (2014).
50. F. Bretzner, R. M. Brownstone, Lhx3-Chx10 reticulospinal neurons in locomotor circuits. *J. Neurosci.* **33**, 14681–14692 (2013).
51. M. Hayashi *et al.*, Graded arrays of spinal and supraspinal V2a interneuron subtypes underlie forelimb and hindlimb motor control. *Neuron* **97**, 869–884.e5 (2018).
52. L. Ye *et al.*, Wiring and molecular features of prefrontal ensembles representing distinct experiences. *Cell* **165**, 1776–1788 (2016).
53. C. B. Mantilla, Y. B. Seven, J. N. Hurtado-Palomino, W. Z. Zhan, G. C. Sieck, Chronic assessment of diaphragm muscle EMG activity across motor behaviors. *Respir. Physiol. Neurobiol.* **177**, 176–182 (2011).
54. C. B. Mantilla, S. M. Greising, J. M. Stowe, W. Z. Zhan, G. C. Sieck, TrkB kinase activity is critical for recovery of respiratory function after cervical spinal cord hemisection. *Exp Neurol* **261**, 190–195 (2014).
55. K. Z. Lee *et al.*, Phrenic motoneuron discharge patterns following chronic cervical spinal cord injury. *Exp. Neurol.* **249**, 20–32 (2013).
56. D. D. Fuller *et al.*, Modest spontaneous recovery of ventilation following chronic high cervical hemisection in rats. *Exp. Neurol.* **211**, 97–106 (2008).
57. D. Komnenov *et al.*, Intermittent hypoxia promotes recovery of respiratory motor function in spinal cord-injured mice depleted of serotonin in the central nervous system. *J. Appl. Physiol.* **121**, 545–557 (2016).
58. H. H. Ellenberger, J. L. Feldman, H. G. Goshgarian, Ventral respiratory group projections to phrenic motoneurons: Electron microscopic evidence for monosynaptic connections. *J. Comp. Neurol.* **302**, 707–714 (1990).
59. H. H. Ellenberger, J. L. Feldman, Monosynaptic transmission of respiratory drive to phrenic motoneurons from brainstem bulbospinal neurons in rats. *J. Comp. Neurol.* **269**, 47–57 (1988).
60. M. G. Zaki Ghali, G. Britz, K. Z. Lee, Pre-phrenic interneurons: Characterization and role in phrenic pattern formation and respiratory recovery following spinal cord injury. *Respir. Physiol. Neurobiol.* **265**, 24–31 (2019).
61. M. A. Lane, Spinal respiratory motoneurons and interneurons. *Respir Physiol. Neurobiol.* **179**, 3–13 (2011).
62. K. Qiu, M. A. Lane, K. Z. Lee, P. J. Reier, D. D. Fuller, The phrenic motor nucleus in the adult mouse. *Exp. Neurol.* **226**, 254–258 (2010).
63. L. V. Zholudeva *et al.*, The neuroplastic and therapeutic potential of spinal interneurons in the injured spinal cord. *Trends Neurosci.* **41**, 625–639 (2018).
64. M. S. Sandhu *et al.*, Respiratory recovery following high cervical hemisection. *Respir Physiol. Neurobiol.* **169**, 94–101 (2009).
65. S. A. Crone *et al.*, Irregular breathing in mice following genetic ablation of V2a neurons. *J. Neurosci.* **32**, 7895–7906 (2012).
66. W. J. Alilain *et al.*, Light-induced rescue of breathing after spinal cord injury. *J. Neurosci.* **28**, 11862–11870 (2008).
67. G. Zhong *et al.*, Electrophysiological characterization of V2a interneurons and their locomotor-related activity in the neonatal mouse spinal cord. *J. Neurosci.* **30**, 170–182 (2010).
68. K. J. Dougherty, O. Kiehn, Firing and cellular properties of V2a interneurons in the rodent spinal cord. *J. Neurosci.* **30**, 24–37 (2010).
69. P. M. Warren *et al.*, Rapid and robust restoration of breathing long after spinal cord injury. *Nat. Commun.* **9**, 4843 (2018).
70. Y. B. Seven, C. B. Mantilla, G. C. Sieck, Recruitment of rat diaphragm motor units across motor behaviors with different levels of diaphragm activation. *J. Appl. Physiol.* **117**, 1308–1316 (2014).
71. V. N. Jensen, *V2a Neurons Pattern Respiratory Muscle Activity in Health and Disease* (University of Cincinnati, 2020), p. 208.
72. H. Zhu *et al.*, Cre-dependent DREADD (Designer Receptors Exclusively Activated by Designer Drugs) mice. *Genesis* **54**, 439–446 (2016).
73. D. A. McCreedy *et al.*, Passive clearing and 3D lightsheet imaging of the intact and injured spinal cord in mice. *Front. Cell. Neurosci.* **15**, 684792 (2021).
74. K. H. Minor, L. K. Akison, H. G. Goshgarian, N. W. Seeds, Spinal cord injury-induced plasticity in the mouse–the crossed phrenic phenomenon. *Exp. Neurol.* **200**, 486–495 (2006).
75. D. E. Becker, Fundamentals of electrocardiography interpretation. *Anesth. Prog.* **53**, 53–63; quiz 64 (2006).